



VYSOKÉ UČENÍ TECHNICKÉ V BRNĚ

BRNO UNIVERSITY OF TECHNOLOGY

FAKULTA STAVEBNÍ

FACULTY OF CIVIL ENGINEERING

ÚSTAV GEOTECHNIKY

INSTITUTE OF GEOTECHNICS

DESIGN OF OFFSHORE COFFERDAM LOADED BY VERTICAL SURCHARGE

NÁVRH KONSTRUKCE SUCHÉHO DOKU POD SVISLÝM ZATÍŽENÍM

DIPLOMOVÁ PRÁCE

DIPLOMA THESIS

AUTOR PRÁCE

AUTHOR

Bc. Simona Zetková

VEDOUCÍ PRÁCE

SUPERVISOR

MICHAL UHRIN

BRNO 2017



VYSOKÉ UČENÍ TECHNICKÉ V BRNĚ

FAKULTA STAVEBNÍ

Studijní program	N3607 Stavební inženýrství
Typ studijního programu	Navazující magisterský studijní program s prezenční formou studia
Studijní obor	3607T009 Konstrukce a dopravní stavby
Pracoviště	Ústav geotechniky

ZADÁNÍ DIPLOMOVÉ PRÁCE

Student	Bc. Simona Zetková
Název	Design of Offshore Cofferdam Loaded by Vertical Surcharge
Vedoucí práce	Michal Uhrin
Datum zadání	31. 3. 2016
Datum odevzdání	13. 1. 2017

V Brně dne 31. 3. 2016

doc. Ing. Lumír Miča, Ph.D.
Vedoucí ústavu

prof. Ing. Rostislav Drochytka, CSc., MBA
Děkan Fakulty stavební VUT

PODKLADY A LITERATURA

- 1) Ground conditions - Report. Drawings.
- 2) Geometrical arrangement - Drawings.
- 3) Design criteria - Design Statement.
- 4) Miscellaneous - Slides from BIM model. Presentations. Project sheets.

ZÁSADY PRO VYPRACOVÁNÍ

Subject:

Structural/geotechnical engineering analysis and design of offshore cofferdam from steel pile wall for reception of immersed tube tunnel. Working platforms supported by the cofferdam in some sections will exert heavy vertical load on the pile wall and thus subject it to 2nd order effects.

Tasks:

- Desk study of inputs and design criteria.
- Internet research of calculation methods (see below).
- Analytical models and calculations.
- Structural design checks.
- Summary of inputs, methodology and outputs / findings / conclusions into formal report.

Items to be addressed:

- General description of the structure;
- Description of construction sequence;
- Description of ground and groundwater conditions;
- Research regarding: Temperature load on steel struts. Second order effects (axial compression of flexible structure deflected from lateral load).
- Analytical models: 1 characteristic section. 2 methodologies - subgrade reaction and geotechnical FEM - structural FEM only if beneficial in some respect. Comparison of results. Structural FEM model of 1 lateral support frame.
- Structural design checks: Steel pile wall in analysed section. 1 lateral support frame (struts and waler beams).

Specifications:

- Consider 2nd order effects on pile wall under vertical compression.
- Consider temperature load on struts.
- Lateral support frame check against disproportionate collapse (accidental loss of single strut).
- Standards: Eurocodes or Hong Kong codes of practice.

Deliverable:

- Report in English language.

STRUKTURA DIPLOMOVÉ PRÁCE

VŠKP vypracujte a rozčleňte podle dále uvedené struktury:

1. Textová část VŠKP zpracovaná podle Směrnice rektora "Úprava, odevzdávání, zveřejňování a uchovávání vysokoškolských kvalifikačních prací" a Směrnice děkana "Úprava, odevzdávání, zveřejňování a uchovávání vysokoškolských kvalifikačních prací na FAST VUT" (povinná součást VŠKP).
2. Přílohy textové části VŠKP zpracované podle Směrnice rektora "Úprava, odevzdávání, zveřejňování a uchovávání vysokoškolských kvalifikačních prací" a Směrnice děkana "Úprava, odevzdávání, zveřejňování a uchovávání vysokoškolských kvalifikačních prací na FAST VUT" (nepovinná součást VŠKP v případě, že přílohy nejsou součástí textové části VŠKP, ale textovou část doplňují).

Michal Uhrin
Vedoucí diplomové práce

ABSTRAKT

Cílem této práce je provést zjednodušený návrh a posouzení suchého doku pod svislým zatížením v rámci virtuálního projektu. Suchý dok postavený v moři musí být schopen přenést všechna působící zatížení po dobu životnosti konstrukce. Jelikož se jedná o dočasnou konstrukci postavenou za účelem výstavby hloubeného tunelu, musí konstrukce splňovat minimální rozměry požadované pro konstrukci tunelu. Návrhová životnost této dočasné konstrukce je pět let. Mezi požadované části práce patří zhodnocení geologických podmínek, naplánování fází výstavby, schéma výstavby příčného řezu, posouzení kritického řezu a rozpěrného rámu. Konstrukce je vystavena velkým teplotním změnám, a proto se v diplomové práci zabývám vlivem teploty na horizontální rozpěry pažících konstrukcí a následně je tento vliv zahrnut v návrhu rozpěr. Dalším požadavkem na práci bylo porovnat výsledky z analytických modelů v programech PLAXIS a GEO5. Rozpěrný rám je řešen zvlášť v programu Scia Engineer. V této práci jsou posuzovány pouze konstrukční prvky ocelová pilotová stěna, rozpěra a převážka. Kvůli svislému zatížení, které působí na již deformovanou konstrukci, jsou pro návrh pilotové stěny uvažovány účinky druhého řádu. Pro jsem se zabývala možnostmi, které máme pro uvažování účinků druhého řádu na ocelové konstrukce. Všechny zmíněné části práce byly zpracovány za pomoci potřebné literatury. Podle statické analýzy konstrukce bylo možné navrhnout konstrukci, která vyhovuje požadavkům na suchý dok pro budoucí stavbu tunelu. Jednotlivé fáze výstavby byly navrženy tak, aby zajistily proveditelnost konstrukce a zároveň minimalizovaly deformace pilotové stěny suchého doku. Jelikož se jedná o konstrukci prováděnou převážně z pracovních plošin, je nutné uvažovat i omezený přístup strojové techniky. Porovnání dvou různých analytických modelů ukázalo výrazné rozdíly mezi programy PLAXIS a GEO5. Posouzení všech konstrukčních prvků bylo provedeno podle Eurokódu 3. Rozpěrný rám je dále posouzen na ztrátu prvku.

KLÍČOVÁ SLOVA

Suchý dok, zatížení teplotou, teorie druhého řádu, pilotová štětová stěna se zámky, rozpěra

ABSTRACT

The aim of this thesis is to undertake simplified design and assessment of cofferdam under vertical surcharge in the form of virtual project. Cofferdam constructed on the sea shore must be able to withstand all loads to enable construction of cut and cover tunnel. As a part of the design it is required to assess ground conditions and it is necessary to review feasibility of the structure on the sea. The construction will be described in construction phases and graphically demonstrated in construction sequence drawing. Because the structure is designed for life time of five years, temperature load on struts is studied in the thesis and further considered in structural analysis. Furthermore, it is required to compare analytical models from GEO5 and PLAXIS. Horizontal frame is analysed separately in Scia Engineer. Structural members – cofferdam wall, waler beam and strut are checked in this thesis. For the design of the cofferdam wall second order theory is considered. All mentioned requirements were accomplished with help of corresponding Eurocodes, books and technical advice. Results of this work are feasible and it was possible to design all members to enable construction of the cut and cover tunnel. The phasing was designed such that deformation of the cofferdam is minimalized and use of machinery is limited to machines on temporary platforms. Comparison of two different analytical models showed that different soil modelling has great effect on internal forces, even though the shape of the bending curve is very similar, values obtained from PLAXIS software are much higher. Assessment of the structural members is done according to Eurocode 3, and horizontal frame is checked also against disproportionate collapse.

KEYWORDS

Cofferdam, temperature load, second order theory, interlocking pipe pile wall, strut

BIBLIOGRAFICKÁ CITACE VŠKP

Bc. Simona Zetková *Design of Offshore Cofferdam Loaded by Vertical Surcharge*. Brno, 2017. 74 s., 6 s. příl. Diplomová práce. Vysoké učení technické v Brně, Fakulta stavební, Ústav geotechniky. Vedoucí práce Michal Uhrin

PROHLÁŠENÍ

Prohlašuji, že jsem diplomovou práci zpracoval(a) samostatně a že jsem uvedl(a) všechny použité informační zdroje.

V Brně dne 3. 1. 2017

Bc. Simona Zetková

autor práce

PODĚKOVÁNÍ

Na tomto místě bych chtěla poděkovat panu Ing. Michalovi Uhrinovi za odborné vedení práce, cenné rady a připomínky, ochotu a vstřícný přístup v průběhu zpracování této diplomové práce. Dále bych chtěla poděkovat zaměstnancům ústavu geotechniky za ochotu a pomoc jak při vytváření této práce, tak i v průběhu studia.

List of Content

1. Project description	4
1.1. Structure description.....	4
1.1.1. Temporary Work Platforms.....	4
1.1.2. Temporary Cofferdam.....	5
1.2. Phase of construction	6
1.3. Design Basis.....	8
2. Geotechnical conditions.....	9
2.1. Geology.....	9
2.1.1. Geotechnical profile along construction site.....	9
2.1.2. Geotechnical Design Parameters	11
3. Temperature load on struts.....	12
4. Structural design.....	15
4.1. Design Loads.....	15
4.1.1. Permanent Loads	15
4.1.2. Variable load.....	16
4.2. Analytical models.....	17
4.2.1. Geology.....	17
4.2.2. Geometry.....	18
4.3. PLAXIS.....	19
4.3.1. Finite Element Mesh	20
4.3.2. Construction Phases.....	20
4.3.3. Wall - internal forces	25
4.3.4. Strut load	27
4.3.5. Deformations	28
4.4. GEO5 Sheeting Check	29
4.4.1. Geology.....	31
4.4.2. Construction phases.....	31

4.4.3.	Wall – Internal forces	31
4.4.4.	Strut load	32
4.5.	Comparison of results obtained in PLAXIS and GEO5 Sheeting Check.....	32
4.6.	Second Order Theory	33
4.7.	Scia Engineer	35
4.7.1.	Solution of the wall	35
4.7.2.	Horizontal frame	38
5.	Structural Analysis	41
5.1.	Interlocking Pipe Pile Wall	41
5.1.1.	Material Properties.....	41
5.1.2.	Cross-sectional properties	41
5.1.3.	Classification of the cross-section.....	42
5.1.4.	Structural Assessment.....	42
5.2.	Waler Beam.....	48
5.2.1.	Material Properties.....	48
5.2.2.	Cross-sectional properties	48
5.2.3.	Classification of the cross-section.....	48
5.2.4.	Structural Assessment – Ultimate limit state	49
5.2.5.	Check against disproportionate collapse.....	53
5.3.	Horizontal Strut.....	58
5.3.1.	Material Properties.....	59
5.3.2.	Cross-sectional properties	59
5.3.3.	Classification of the cross-section.....	59
5.3.4.	Structural Assessment – Ultimate limit state	60
5.3.1.	Check against disproportionate collapse.....	65

Introduction

Work is dealing with a simplified design of a virtual project of temporary cofferdam built in the sea under heavy vertical surcharge. In the beginning, detailed structure description and site set up is summarized to familiarize the reader with local conditions and the project.

Geology is important for the technology and design of the cofferdam. Geotechnical conditions are described according to provided geotechnical investigation report. However, geology changes along the structure, for the aim of this thesis critical section was chosen and most unfavourable geological profile is assumed.

Geometry of the cross-section is simplified and suitable analytical models are created. Critical section is modelled in software PLAXIS and GEO5 Sheeting Check. Lateral support frame is modelled in Scia Engineer. All possible loads affecting the structure are taken into account. Load cases and their combination are calculated with respect to applicable Eurocodes.

One of the specific load case acting on the structure is temperature change affecting axial load in strut. This issue is discussed further in chapter temperature load on struts.

Another characteristic of this structure is transfer of heavy vertical load onto horizontally deformed cofferdam wall. Discussion on second order theory is made and problems considering non-linear modelling that occurred in the design are described.

Design and checks of structural elements – interlocking pipe pile wall, waler beam and horizontal strut are calculated.

1. PROJECT DESCRIPTION

In order to execute cut and cover tunnel several temporary structures need to be constructed. Design of offshore cofferdam loaded by vertical surcharge is a design of temporary structure providing future execution of the tunnel. The structure is designed for a life time of five years. The project consists of design of Temporary work platforms and design of temporary cofferdam. Temporary cofferdam is approximately 150 *meters* long, 22 *meters* wide and up to 25 *meters* deep. In this thesis, only design of the temporary cofferdam is addressed.

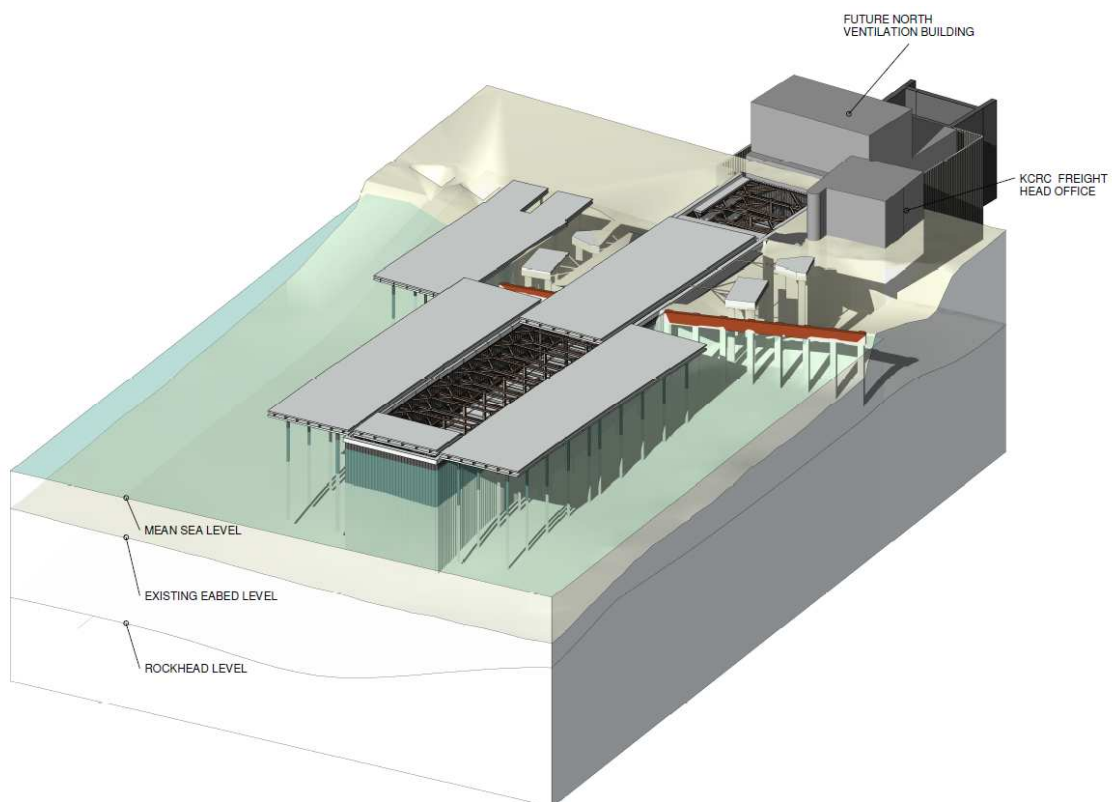


Figure 1.1 Site Setup [1]

For drawings of plan layout and addressed cross-section of the structure please see Annex A.1.

1.1. Structure description

1.1.1. Temporary Work Platforms

Temporary platforms serve for executing driven pipe piles of cofferdam in first stage and provide access for the construction of the temporary cofferdam in second stage.

The temporary platforms are constructed from steel substructure (beams, piles/columns) with a precast concrete deck panel system.

There are two types of temporary platforms:

- Temporary Work Platform above the cofferdam
- Temporary Work Platforms placed in sea

Temporary platform above the cofferdam is designed with substructure made by longitudinal and transversal beams and vertical supporting piles in first stage – before the cofferdam is completed. After the stage is completed vertical piles supporting the platform will be cut off and structure will be transferred on cofferdam pipe piles. There are two platforms of this type:

- The platform placed on the North end of cofferdam which reaches landfall at the existing seawall.
- The platform placed on the South end of cofferdam.

Solution of these platforms will not be included in this thesis.

1.1.2. Temporary Cofferdam

There are several possibilities in construction of temporary cofferdam. As far as the structure needs to be tight we can choose from various types of steel sheet piling or system of interlocking pipe piles. To ensure tightness the interlock would be grouted and in this particular case of offshore cofferdam it would be necessary to use predrilling of granite in order to drive sheets or pipe piles at least half meter into the rock and lock it via pipes into the rock in order to secure position of the wall. Because of the high vertical load and easier feasibility, the interlocking pipe piles are used in the design. Interlocking pipe piles will be used in the harbour and extending 8 m into land beyond the seawall, which is the area considered in the design, and pipe piles with a grout curtain behind in typical landside areas.



Figure 1.2 Construction of Interlocking Pipe Pile Wall [2]

1.2. Phase of construction

Construction must be done in several stages. The project need several temporary structures to be erected prior the structure itself.

At first it is necessary to build working platforms that will be used for drilling and erection machines for the cofferdam walls. Furthermore, fender piles protecting the bridge piers need to be temporarily removed. All these preparation works are done from barges.

Once the preparation structures are built the erection of the cofferdam may begin.

Second stage is construction of interlocking pipe pile walls – predrilling into the granite is provided from temporary platforms along the structure. The average depth of loosening is about 0.7 m. The interlocking piles will be secured with grouted shear pins into the granite and this should secure the wall from toe movement and mostly ensure water tightness. Interlocks are for higher performance grouted.



Figure 1.3 Detail of the interlock [2]

In third stage first strut level S1 is installed together with the walling beam. Then the inside of the cofferdam is dewatered 1.0 *m* below the second strut level, so that the second strut level can be installed. Additionally, pumping test should be executed to verify the effectiveness of the cut of.

In fourth stage, we carry on in dewatering 1.0 *m* below the third strut level S3 and install strut level S3.

In fifth stage, we get to the depth of the sea bed. Dewater 1.0 *m* below the excavation level and excavate 0.5 *m* below the fourth strut level S4. Then install the strut level S4.

Sixth stage is analogical to fifth stage with the next strut level S5 and continues to final excavation level and dewatering 1.0 *m* below this level.

In the last seventh stage the platform is adjusted so that it vertically loads the cofferdam and original supporting piles of the temporary platform can be removed.



Figure 1.4 Pile Works on the Sea [3]

Please see graphical solution in Annex A2.

1.3. Design Basis

In this project, we are dealing with geotechnical structure, therefore load design values and combination are calculated according to Eurocode 7. For this type of structure design approach 2 was chosen. All structural members are made of steel. Therefore, assessment will be calculated according to Eurocode 3.

2. GEOTECHNICAL CONDITIONS

2.1. Geology

In area of Temporary Cofferdam, the geological stratigraphy is represented by layer of marine sand, below located layer of alluvium and then layer of material decomposed from the solid geological strata. Some anthropogenic deposits and man-made material are overlying the natural seabed.

2.1.1. Geotechnical profile along construction site

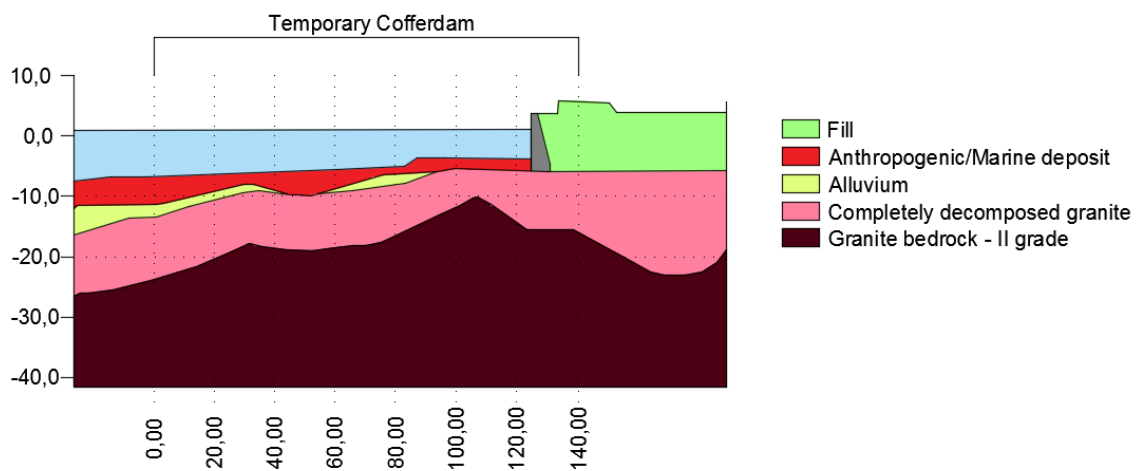


Figure 2.1 Geotechnical Profile

Above mentioned strata could be described as:

- Marine Deposit or Anthropogenic Deposit – described as very soft to soft, grey or black with dapped colour, slightly sandy to silty clay

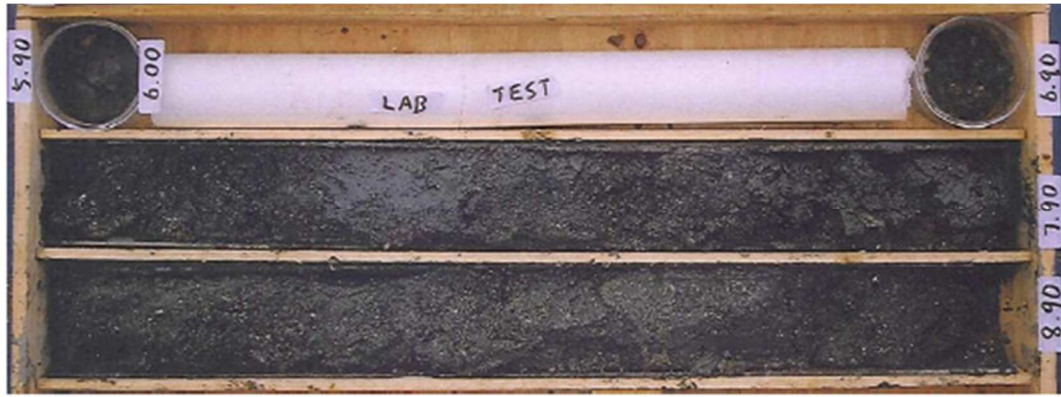


Figure 2.2 Anthropogenic Deposit

- Alluvium – consist of light grey to grey and brown mottled red and yellow, lightly to moderately over-consolidated sandy silt/clays, silty/clayey sands and clean shelly sands with some possible interbed of clay and local gravel and cobble beds



Figure 2.3 Triaxial Specimen of Alluvium

- Completed Decomposed Granite – consist of firm sandy silt/clay to silty/clayey fine to medium sand
- Granite Bedrock - Grade II granite



Figure 2.4 Granite Samples

The onshore part of the site is covered by layer of fill. Marine deposit and alluvium are absent or relatively thin in this area. Offshore part of the site is generally underlain by anthropogenic deposit or marine deposits. These layers are placed above the layer of alluvium or placed directly on completely decomposed granite. Lower situated is Granite rock head.

For the onshore section, the groundwater level lies between 2 m and 4 m below existing ground level.

Only offshore structure is designed in this thesis.

2.1.2. Geotechnical Design Parameters

Geotechnical parameters are taken from geotechnical report. [1] These parameters were obtained in laboratory and in field tests.

Table 2.1 Geotechnical Parameters

Material	γ_{unsat} [kNm ⁻³]	γ_{sat} [kNm ⁻³]	c' [kPa]	ϕ' [°]	E' [MPa]	ν'	K_0	R_{int}	Condition	Material model
MD/AD	16	18	0	30	8	0.2	0.5	2/3	Drained	M-C ¹
Alluvium	18	20	0	30	8	0.2	0.5	2/3	Drained	M-C
CDG	18	20	5	35	27.5	0.2	0.5	2/3	Drained	M-C
Granite	24	24	-	-	3300	0.3	0.4	2/3	Non-porous	L-E ²

¹ M-C stands for Mohr Coulomb material model

² L-E stands for Linear Elastic material model

3. TEMPERATURE LOAD ON STRUTS

Temperature load on strut is another task to be discussed in my thesis. Because temperature may affect axially loaded members it should be examined how big is the effect on the strut in the horizontal frame in the cofferdam. Temperature load can have either axial effect – that is in case that the load is uniform in the cross-section, or bending effect which occurs when member is warmed or cooled from one side more than from the other. The bending effect would not be considered in this study.

Temperature changes may cause significant changes in strut loads and therefore should be considered in the design of strutted excavation. Temperature load in struts is influenced mostly by the weather, there is not only difference between day and night, winter and summer temperatures but thermal effect can be also caused by sunlight which can evoke eccentric loading in the strut. From elasticity, we know formula for load calculation induced by change in temperature

$$P = \alpha EA \Delta t$$

where

αcoefficient of thermal expansion

Eelastic modulus of steel

Aarea of strut

Δtchange in temperature.

From there it is easy to see that in case that structure is restraint load caused by temperature is not dependent on the length of the strut. However, if we speak about sheeting in soils, it is more likely that structure will deflect and axial load change will be dependent on the stiffness of the structure and therefore on the length of the strut.

But the question is how to apply this knowledge in field of struts. Or generally, in the field where the site setup cannot be assumed to follow elastic principles anymore. From the elastic formula for load caused by temperature change we can learn that this force is not dependent on length of the prop, but as it can be noticed that the larger cross-section of the prop we have the larger force is induced by the same temperature change. Therefore, using more steel to resist thermal loads actually generates more thermal load. In this basic

formula, the strut is assumed fully restrained, which would hardly be realistic. And that might be the main problem - how to estimate the level of restraint.

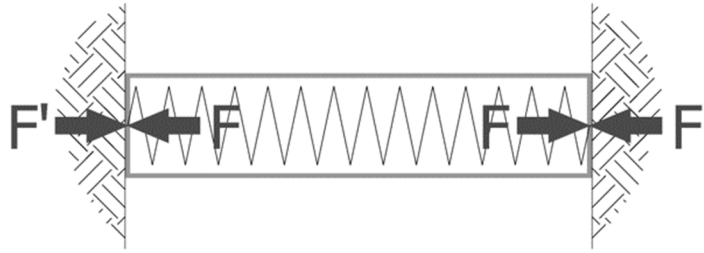


Figure 3.1 The strut is fully restrained by rigid supports and all the potential expansion from temperature effects is translated into extra axial load. [4]

Several measurements of this effect were taken around the world in order to estimate local conditions and probably some possible empirical calculation of the temperature effect. So far, we know that load change depends on cross-sectional area, elastic modulus, coefficient of thermal expansion, change in the temperature and on boundary conditions.

In the study of performance of a braced excavation in granular and cohesive soils, which was performed in Washington D.C., it was determined that there is specific relation between the temperature change and load in a strut. [5] In this study, use of high accuracy extensometers permitted comparison of the loads and deflections resulting from temperature changes and that provided an opportunity to estimate a modulus for the soil behind the wall. By combining the relation for elastic displacement of the cut wall with the effect of temperature on load and displacement of a strut following relation is obtained

$$\Delta P = \frac{A_s E_s \alpha \Delta T}{1 + \frac{3nA_s E_s H}{A_w E L}} \quad [kN]$$

where

E_selastic modulus of steel

αcoefficient of thermal expansion

ΔTchange in temperature

nA_stotal area of struts acting against the wall of area A_w

A_wcut of area of the wall

Esoil modulus of deformation

Llength of the strut

The soil modulus of deformation can be estimated by using relation given in several references for a uniform pressure applied over a rectangular area on an elastic half-space.

$$E = \frac{1,5H(1 - \nu^2)P}{\delta}$$

where

Hheight of the wall

νPoisson's ratio

Paverage load applied over the area of the wall

δdeflection of the wall due to the load change

From the formula of load change calculation, it can be derived that strut load changes will approach load changes for restrained strut if either the soil modulus is high or the ratio nA_s/A_w is quite low or the length of the strut is great with respect to the cut height.

This empirical solution seems reasonable to me and its application does not require complex software. Another way of defining temperature load on strut is to model whole problem in FEM or other software, which can be very complicated. There it is necessary to pay attention to many facts as modelling correct boundary conditions and all connections.

4. STRUCTURAL DESIGN

Structure will be solved in critical section where the depth of rock head is about 24 m. The calculation will provide design of interlocking pipe wall, horizontal frame - waler beam and struts. Critical section is marked in the Figure 4.1 as AA'.

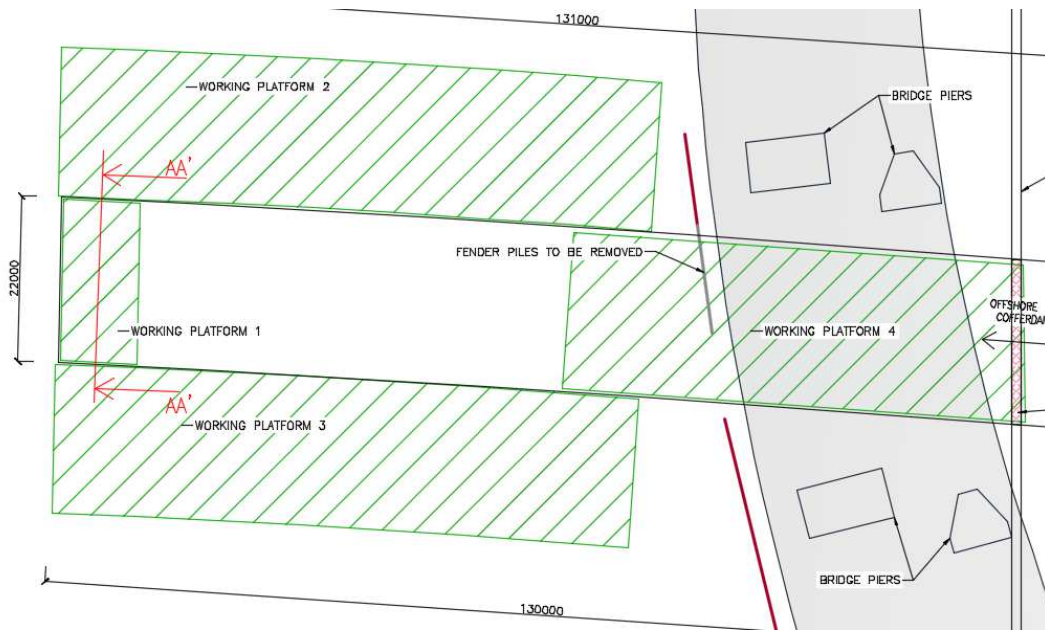


Figure 4.1 Critical Section - Ground plan

Structure will be calculated in software PLAXIS, GEO5 and second order effects will be verified in Scia Engineer according to Eurocode 3. Horizontal frame will be solved in Scia Engineer.

4.1. Design Loads

4.1.1. Permanent Loads

Self-weight – LC1

- Reinforced concrete $\gamma_c = 24.5 \text{ kNm}^{-3}$
- Structural steel $\gamma_s = 78.5 \text{ kNm}^{-3}$

Imposed dead load – LC2

Load from the working platform.

Platform is assumed 1.5 m thick, 22 m long. An average value is taken, the platform is assumed as reinforced concrete even though there will be precast panels together with steel beams.

Lateral earth pressure – LC3

All calculation of lateral earth pressures will be carried out by geotechnical software (GEO5 and PLAXIS) on the base of soil parameters (Table 2.1 Geotechnical Parameters).

Water pressure – LC4

Mean water level will be assumed in the design.

Table 4.1 Design Sea Water Level

Level Type	Sea Level (mPD)	Weight (kN/m ³)
Mean Sea Level	+1.3	10.25

4.1.2. Variable load

Construction Load – LC5

Load that acts on working platform. This load should represent all machinery and materials stored and transferred on the platforms. The highest value is given by weight of the piling rig, which is 40 kNm⁻². This value will be assumed over whole area of the working platform.

Wave forces on vertical structures – LC6

According to Port Work Design Manual the maximum wave force on the cofferdam is $F = 16.7 \text{ kNm}^{-1}$, where temperature is assumed 20°C. This force act horizontally 0.3 m above the mean sea level.

Temperature load – LC7

The reference temperature is assumed 20°C. The positive temperature difference will create additional load in the struts, therefore only positive difference is assumed in the design. Maximum positive temperature difference ΔT is 25°C. This was given in the assignment of the virtual project.

4.2. Analytical models

Structure is modelled analogically in two geotechnical software's – PLAXIS and in GEO5. For the analysis of horizontal frame software Scia Engineer is used.

PLAXIS 2D	Geotechnical FEM - finite element package intended for two-dimensional analysis of deformation and stability in geotechnical engineering and rock mechanics.
GEO5 Sheeting Check	The program verifies the input structure using the method of subgrade reaction. The load applied to the structure is derived from its deformation, which allows to realistically model its behaviour.
Scia Engineer	Structural FEM – soil is substituted by spring supports of calculated stiffness.

4.2.1. Geology

From the geological profile, I estimated average geological strata for the critical section. Strata are assumed to run horizontally. The depth of granite is assumed to be 23.7 m at the critical section.

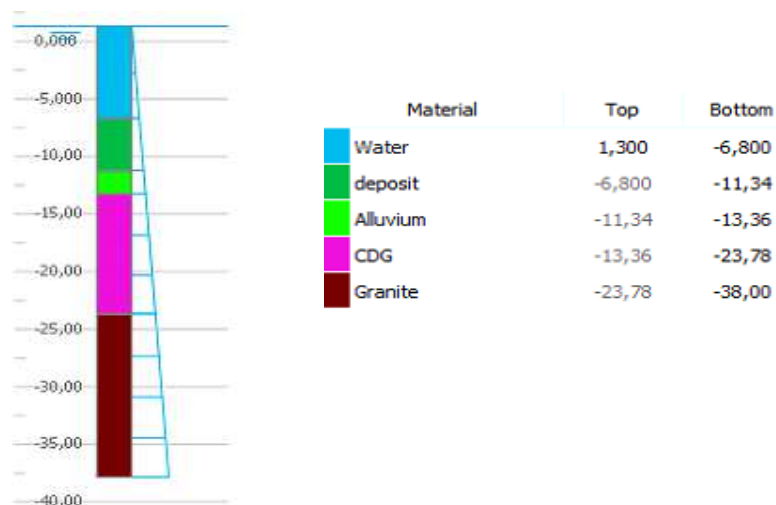


Figure 4.2 Geological Profile

4.2.2. Geometry

The wall is assumed 28.2 m height with its top at 3.8 m and toe at -24.4 m. In the modelling, it was also tested whether it would affect solution if the structure was only in contact with granite. It did not have almost any influence on deformations, however it had significant influence on internal forces and furthermore I think that it would influence water behaviour. If the wall was not drilled into the granite large water inflows should be considered in to the cofferdam and seepage should be modelled. If the wall was only touching the granite head the bending moment will be less, because the soil above is not as strong and does not evoke such forces. It is a question how deep can be the piles driven – if they are driven too deep, the internal forces reach very high values, if they are not driven enough the wall would not be as water tight as required. I supposed in a design that the piles will be driven with the help of predrilling to 0.7 m into the granite and the bottom will be grouted with the shear pin.

Preliminary design of structural elements

- Interlocking pipe pile wall - $\Phi 700/16$ mm
- Strut level S1 - CHS 508/16 mm
- Strut level S2 – CHS 660/30 mm
- Strut level S3 – CHS 1016/32 mm
- Strut level S4 – CHS 1016/32 mm
- Strut level S5 – CHS 762/30 mm
- Waler beam – PI Chamber 600/500 mm

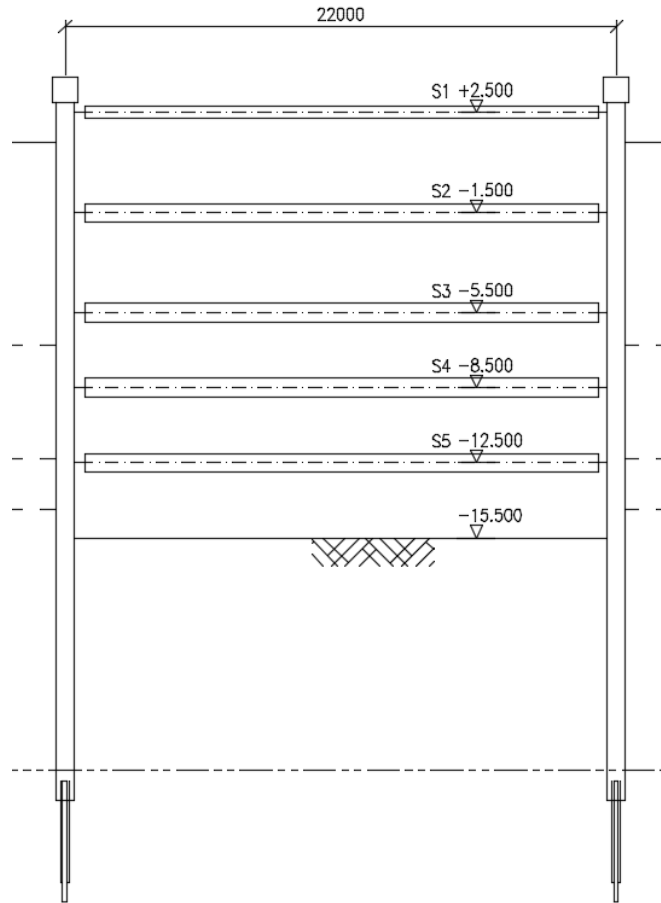


Figure 4.3 Strut Levels

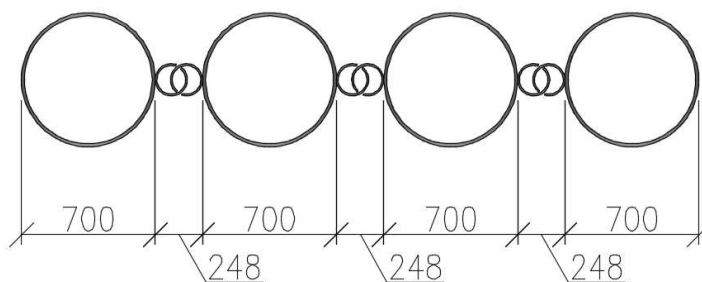


Figure 4.4 Interlocking Pipe Pile Wall

4.3. PLAXIS

Using software PLAXIS I carried out calculation of the structure using finite element method. I used software PLAXIS 2D and for the mesh 15-nodes triangular elements are used. All structural members are modelled by element type Plate (linear elastic material model). Soils

were modelled by Mohr-Coulomb material model and granite is represented by linear elastic material model. Interfaces between the soil and structure is adjusted with reduction factor $R_{inter} = 0.67$.

4.3.1. Finite Element Mesh

The mesh is generated as medium refined symmetrically around the structure.

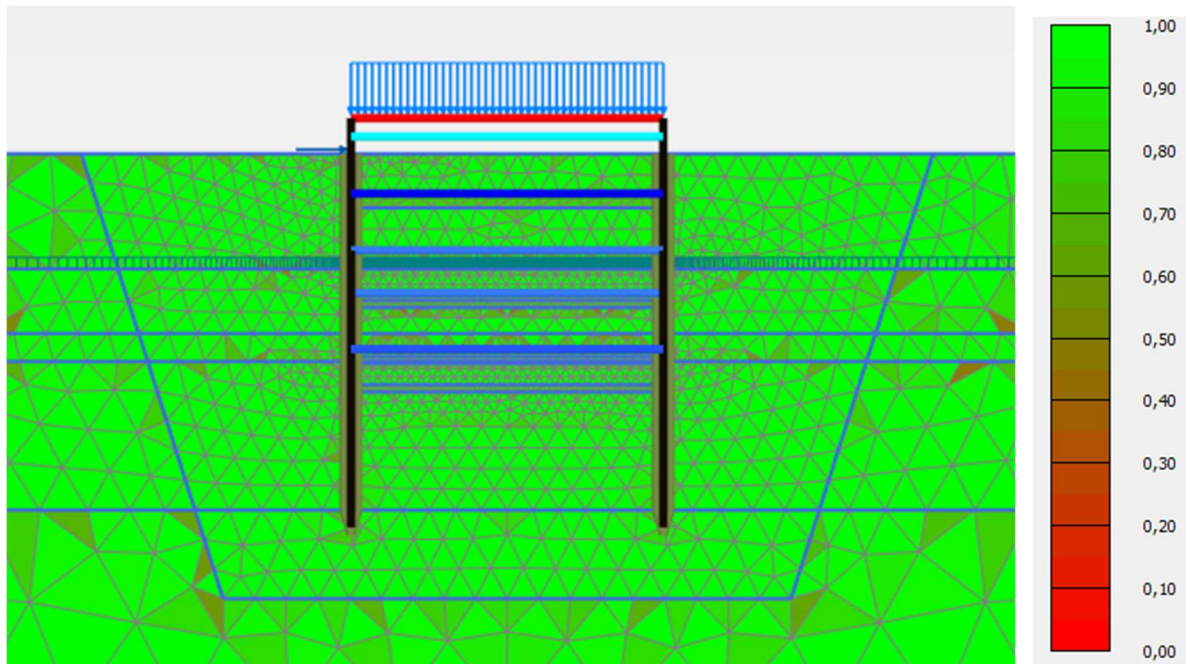


Figure 4.5 Mesh Quality

4.3.2. Construction Phases

Construction phases are shown in following Figures 4.5 – 4.13. Except from representation of work done in each phase, pictures show contours of soil deformation.

Initial Phase – undisturbed geology, no structures activated

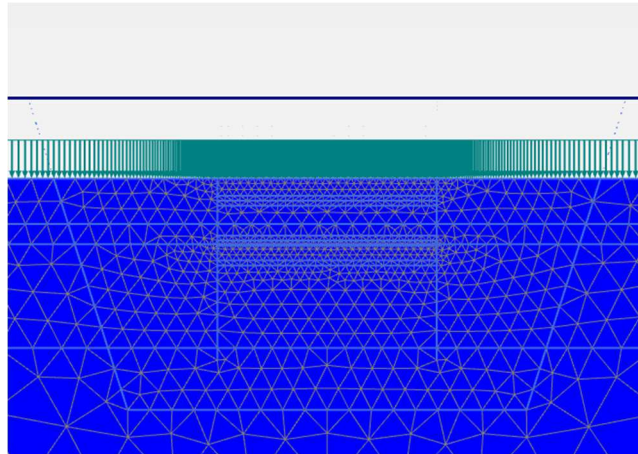


Figure 4.6 Initial Phase

First Phase

Activation of interlocking pipe pile walls. There is water acting on the pipe pile wall. Displacements are zero in this phase.

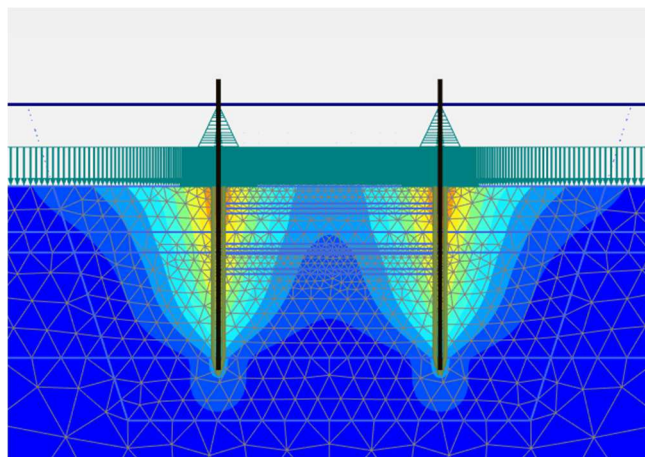


Figure 4.7 Phase 1

Second Phase

First pumping phase, water is decreased inside of the cofferdam from 1.3 m to -2.5 m and the first strut level is installed at +2.5 m. Maximum ground deformation is 0.06 m.

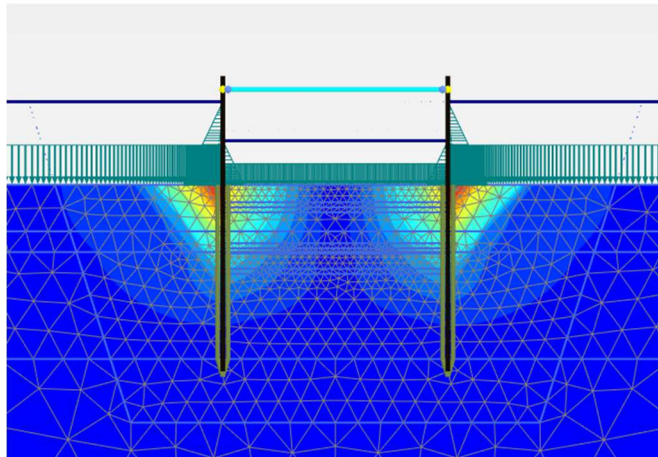


Figure 4.8 Phase 2

Third Phase

Installation of the second strut level at -2 m and further water pumping to -6.5 m . Maximum deformation in this phase reaches value 0.1 m . Already in this phase we can observe plastic behaviour of the soil. The soil deformation is significant in this phase but would not rise further more in following phases.

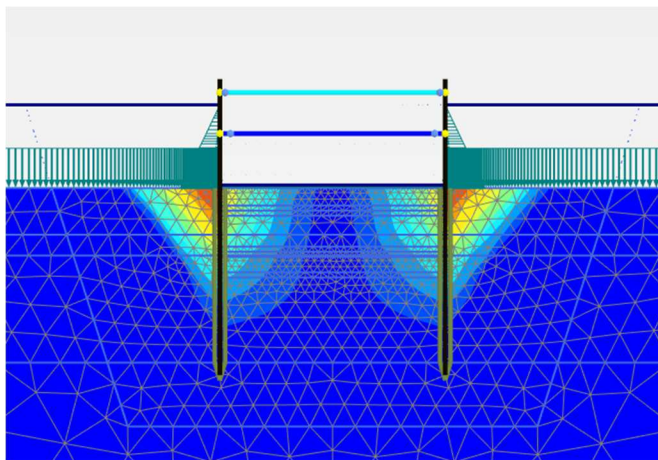


Figure 4.9 Phase 3

Fourth phase

Third strut level at -5.5 m is activated and water is pumped to -9.5 m . Soil is excavated to -9.0 m . Maximum ground deformation rises to 0.11 m .

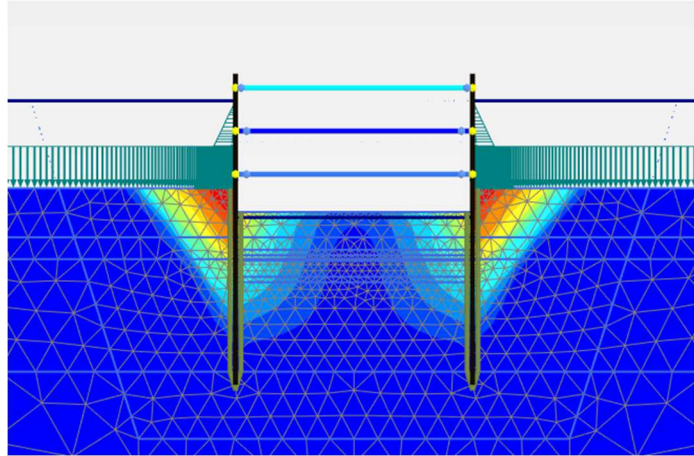


Figure 4.10 Phase 4

Fifth Phase

Activation of the strut level S4 at -8.5 m and further pumping to -13.5 m . Excavation is done to -13.0 m . Maximum ground deformation exceeds 0.14 m .

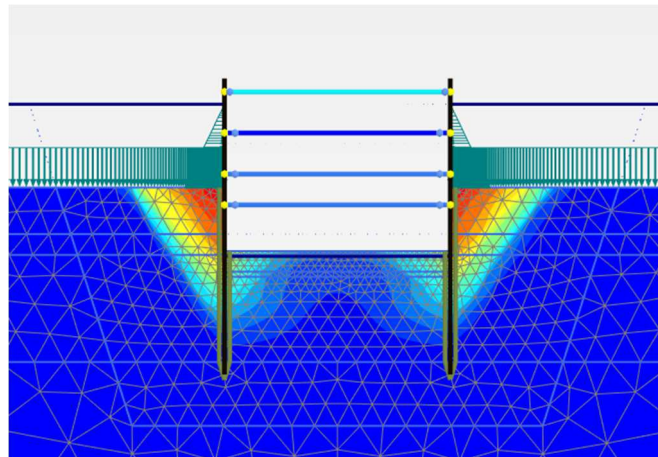


Figure 4.11 Phase 5

Sixth phase

Last excavation phase. Last strut level S5 at -12.5 m is activated and water is pumped to -15.5 m and soil is excavated to its final level -15.0 m . Maximum deformation does not exceed 0.15 m .

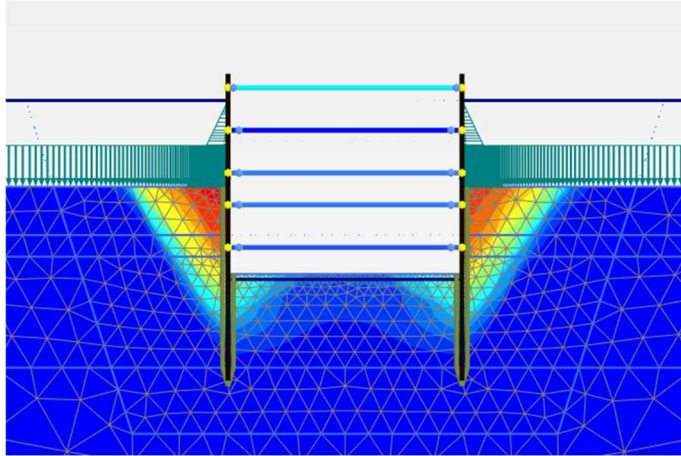


Figure 4.12 Phase 6

Seventh Phase

In this phase is the temporary platform and the load on it activated.

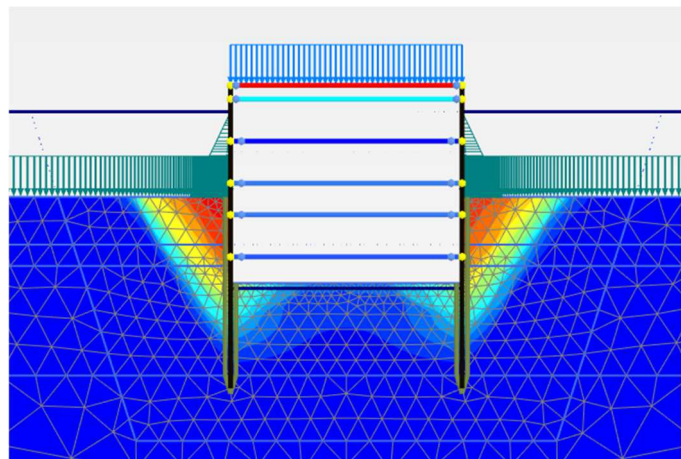


Figure 4.13 Phase 7

Eight Phase

In this last construction phase is wave force applied on the left side of the cofferdam. The wave load could theoretically act in all construction phases, but for simplification is was applied in the end when the internal forces reach highest values.

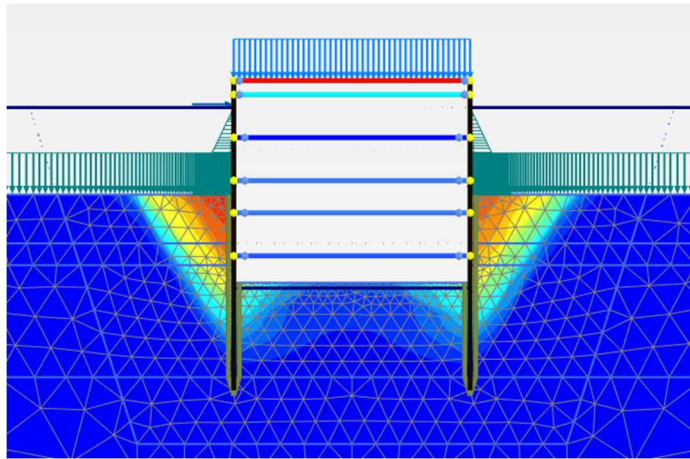


Figure 4.14 Phase 8

4.3.3. Wall - internal forces

Bending Moments

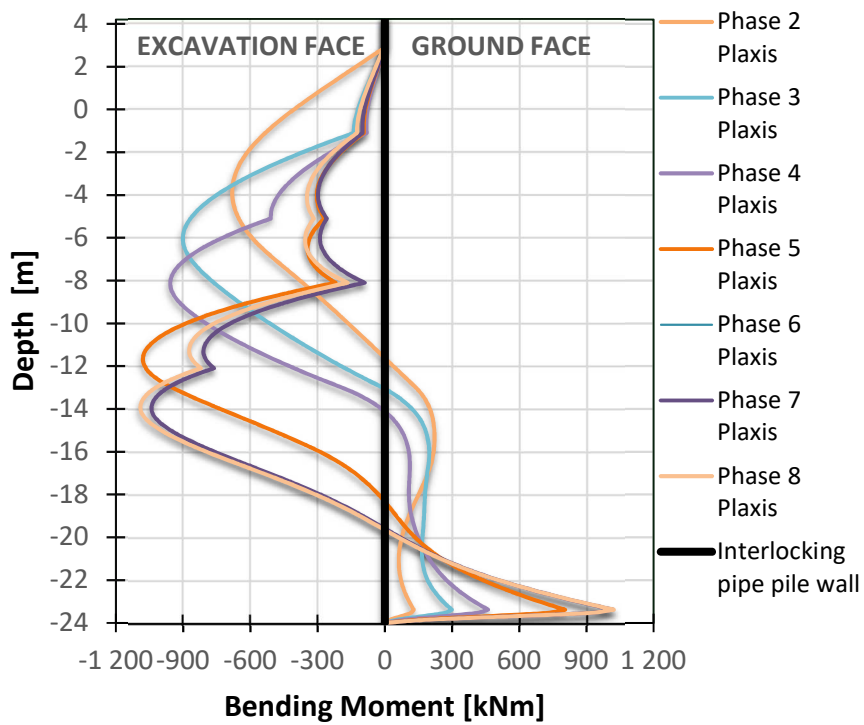


Figure 4.15 Bending Moment Diagram

Maximum bending moment along the wall can be observed in phases 7 and 8. These values will be considered in wall design.

Axial Force

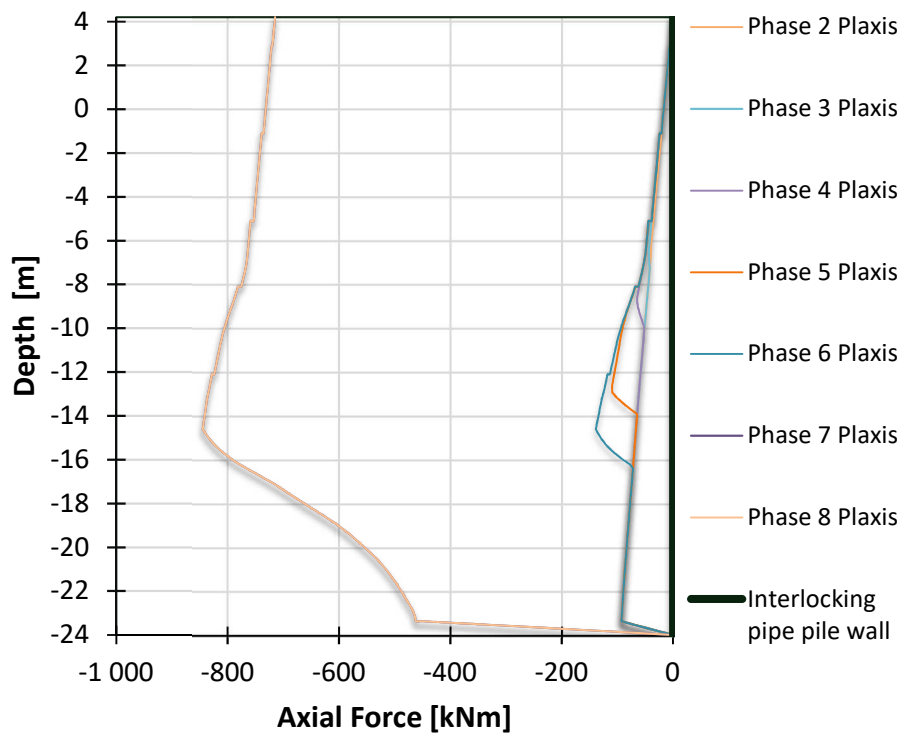


Figure 4.16 Axial Force Diagram

In eight phase, we can observe much higher values of the axial force than in all previous phases. This is caused by transferring the load from the working platform onto the cofferdam wall's.

Shear Force

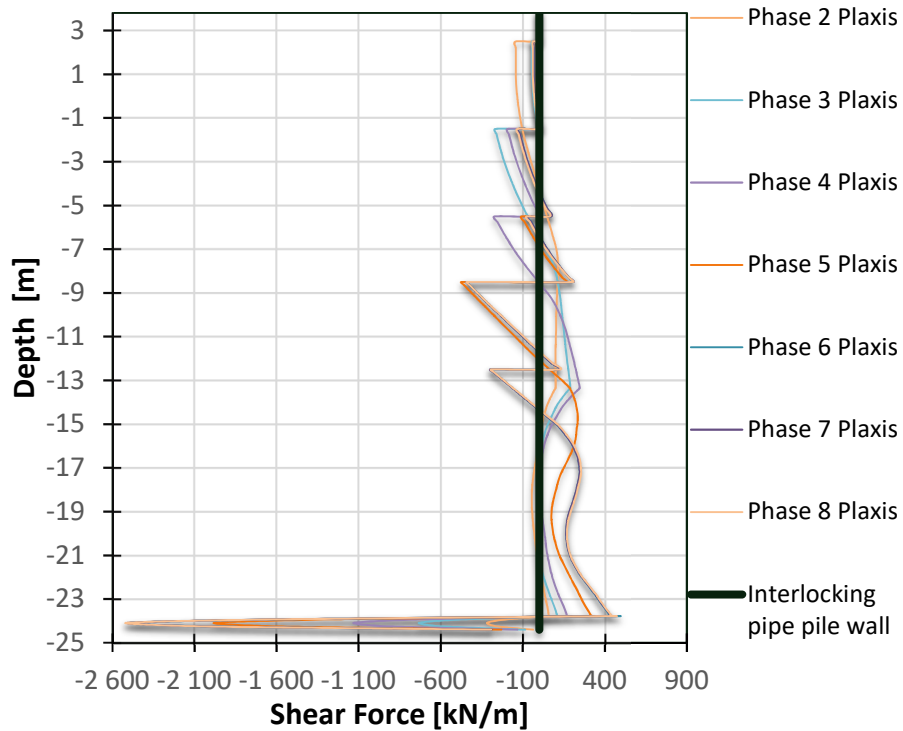


Figure 4.17 Shear Force Diagram

Highest values are reached at the toe of the structure, where the wall is rigidly embedded into the granite.

4.3.4. Strut load

Maximum axial force in strut occurred in strut SL4 in sixth phase of construction. The value is 647 kN/m , giving force 5176 kN in one strut S4 if we assume strut spacing 8 m .

Table 4.2 Axial force in Strut levels in each phase [kN/m]

	Phase 2	Phase 3	Phase 4	Phase 5	Phase 6	Phase 7	Phase 8	Max
SL1	142.8	44.2	29.6	32.7	34.2	34.2	35.7	142.8
SL2	–	262.8	202.4	136.0	130.6	130.5	134.1	262.8
SL3	–	–	277.3	174.8	138.4	139.4	139.5	277.3
SL4	–	–	–	639.1	645.0	647.0	646.5	647.0
SL5	–	–	–	–	414.8	417.9	421.3	421.3
Max	142.8	262.8	277.3	639.1	645.0	647.0	646.5	647.0

4.3.5. Deformations

Maximum wall deformation

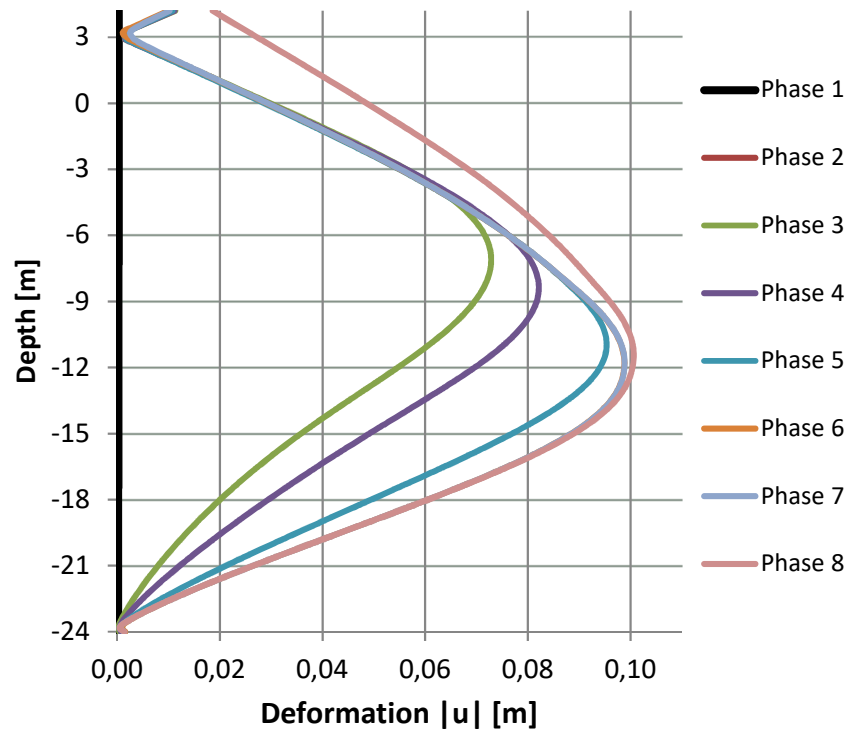


Figure 4.18 Wall deformation

Plastic straining

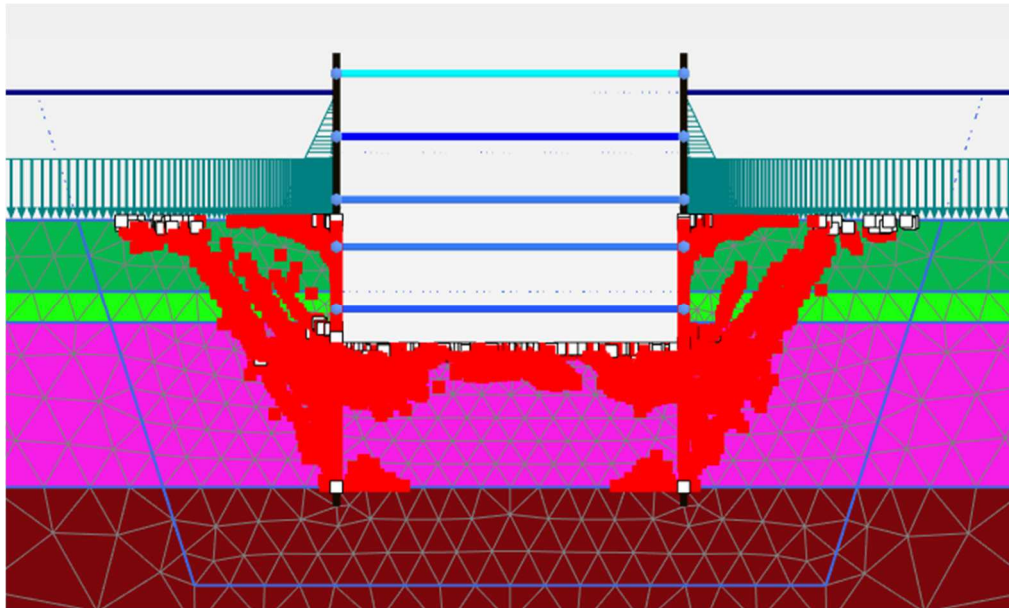


Figure 4.19 Plastic points

From this plastic point interpretation, we can see that the soil overlaying granite is weak. Figure 4.19 Plastic points shows where the stress exceeds elastic capacity of the soil. Therefore, it can be expected that stress will drop close to active lateral earth pressure at the ground face. On the excavation face, less plastic points occurred, which would lead to shift from lateral earth pressure at rest towards passive lateral earth pressure.

4.4. GEO5 Sheeting Check

Software GEO5 uses calculation method of subgrade reaction. The basic assumption of the method is that the soil or rock near the wall behaves as ideally elastic-plastic Winkler material. [6] This material is defined by the modulus of subsoil reaction k_h , which characterizes the deformation in the elastic region and by additional limiting deformations. When exceeding these deformations, the material behaves as ideally plastic.

The concept of this method is based on fact that pressure acting is dependent on deformation.

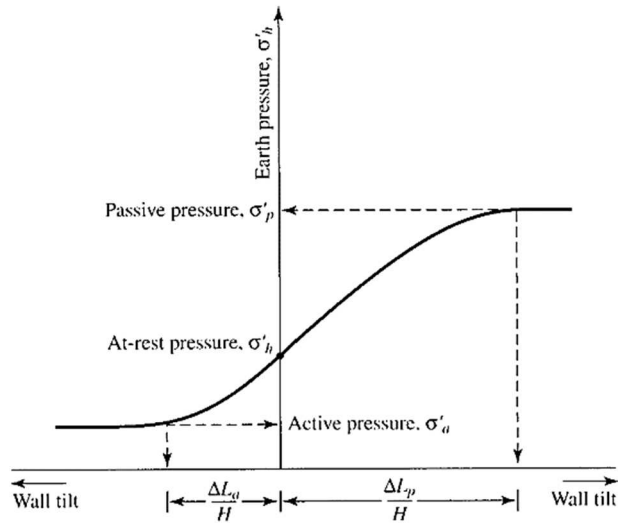
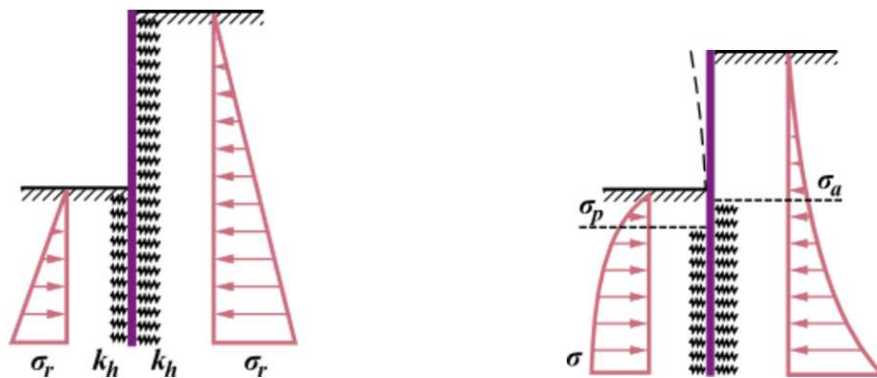


Figure 4.20 Variation of the magnitude of lateral earth pressure with wall tilt [7]



Scheme of structure before first iteration Scheme of structure during the iteration process

Figure 4.21 Subgrade reaction method [6]

I used module Sheeting Check of the GEO5 software for the calculation. As for the general setting I used calculation according to Eurocode 7 Design approach 2. Modulus of subsoil reaction was calculated according to Schmitt, where the analysis builds on the relation between oedometric modulus and bending stiffness of the structure. Modulus of subsoil reaction introduced by Schmitt [8]

$$k_h = 2.1 \frac{E_{oed}^{4/3}}{(EI)^{1/3}}$$

Where

E_{oed}oedometric modulus [MPa]

EIbending stiffness of the structure [MNm²/m].

4.4.1. Geology

I used the same assumptions as in PLAXIS, and applied same ground layers in here. It is a bit tricky how to describe correctly the structure because GEO does not allow us to model protruding structure. Therefore, water was modelled as a soil and in terrain arrangement behind the wall was designed in maximal slope till the sea bed. Afterwards the water level was modelled adequately to real structure.

Soil parameters were entered according to geotechnical report. [1]

4.4.2. Construction phases

In GEO5 were phases modelled analogical to PLAXIS, but in GEO5 we cannot apply axial forces to the wall. Therefore, load from the platform and platform itself is not considered here. In GEO5, I have modelled six phases of construction. First phase in GEO5 correspond to second phase in PLAXIS.

4.4.3. Wall – Internal forces

Bending Moments

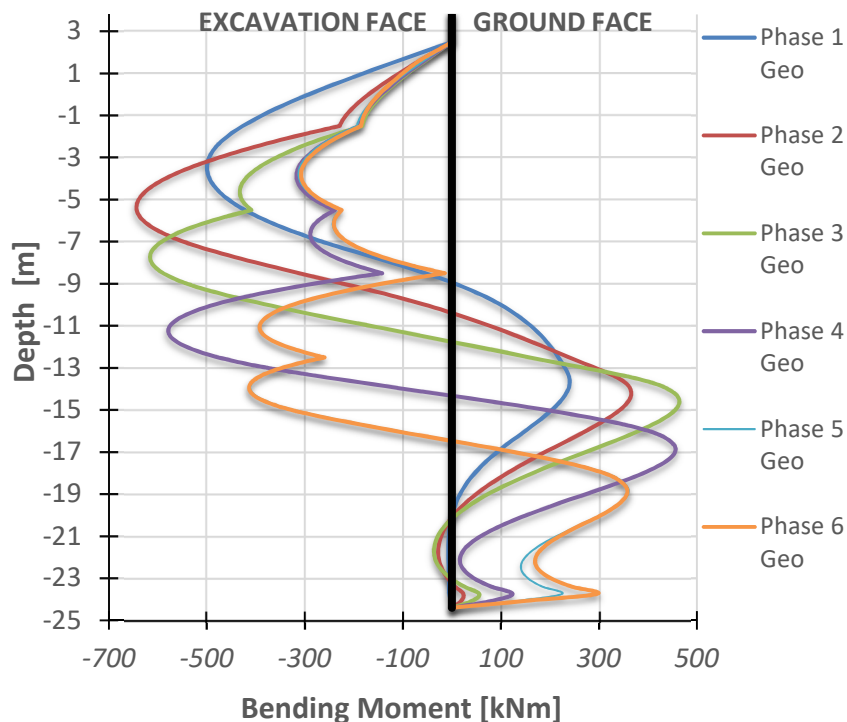


Figure 4.22 Bending moment diagram

There we can see how the moment changes during construction phases. Maximum moment is reached already in the second phase but this maximum value is reached in almost every phase. The values of the bending moment reached in this software are less than values obtained in PLAXIS.

4.4.4. Strut load

The maximum load in strut occurred in fifth phase of construction in S4 with a value of 3895.33 kN.

Table 4.3 Axial force in Strut in each phase [kN]

	Phase 1	Phase 2	Phase 3	Phase 4	Phase 5	Phase 6	Max
S1	1002.3	612.8	519.6	530.4	542.4	628.2	1002.3
S2	–	1369.8	1090.5	728.7	682.3	742.5	1369.8
S3	–	–	1866.9	1480.6	1205.7	1199.6	1866.9
S4	–	–	–	3764.2	3895.3	3890.3	3895.3
S5	–	–	–	–	3172.9	3182.7	3182.7
Max	1002.3	1369.8	1866.9	3764.2	3895.3	3890.3	3895.3

4.5. Comparison of results obtained in PLAXIS and GEO5 Sheeting Check

Bending Moment Comparison

In comparison of the bending moment from PLAXIS and bending moments from GEO5 I noticed that the shapes of the bending moment correspond to each other, however with rising value PLAXIS gives higher values of the bending moment. This can be caused by the different soil models where PLAXIS used Mohr-Coulomb material model with ideal plasticity and in GEO5 the soil is substituted by springs defined by subsoil modulus k_h .

In final phase before transferring the platform onto the cofferdam walls reach the values in PLAXIS 1000 kNm/m from the outside of the wall and 1100 kNm from the inside values from GEO5 are almost half less at the points of extreme. On the top part of the wall, where the soil does not act, the bending curves almost copy each other.

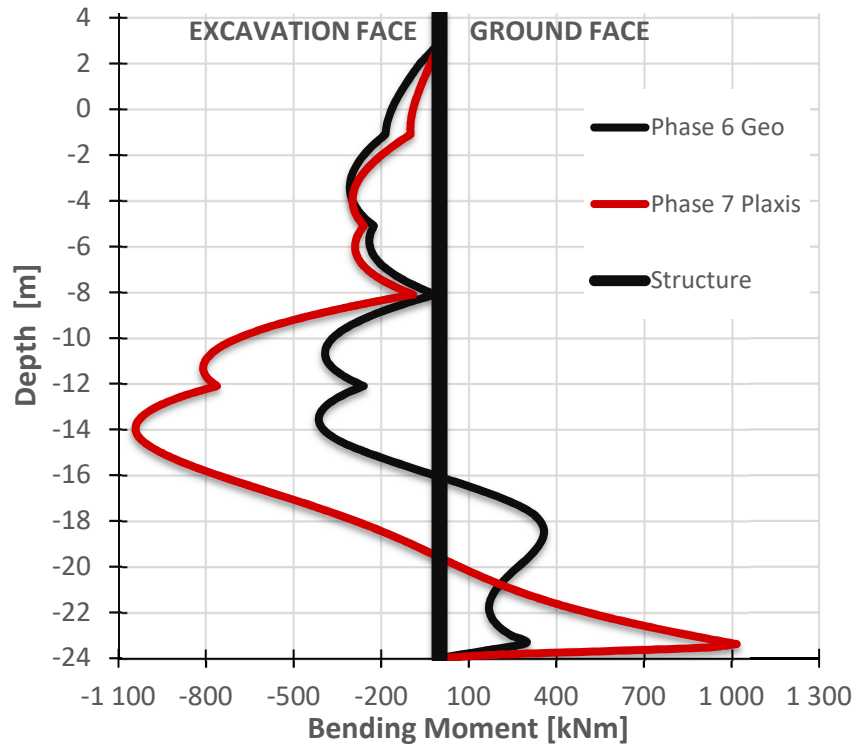


Figure 4.23 Bending Moment Comparison

All comparisons are done in characteristic values. All phases are shown in Annex B1.

4.6. Second Order Theory

Having a deflected steel structure loaded by vertical force leads us to discussion whether the second order effect should or should not be considered. There are three possibilities how to calculate this problem and now I will try to describe all of them. Because we are talking about steel structure all calculations are controlled by and described in Eurocode 3 designated for steel structures design. [9]

1. First order theory – means using initial geometry of the structure. This can be used for the global analysis, if the increase of the relevant internal forces and moments caused by the deformations according to the first order theory is less than 10%. This is fulfilled if the ratio of the elastic critical force for the relevant buckling mode to the design value of the compression force.

$$\alpha_{cr} = \frac{N_{cr}}{N_{Ed}} \geq 10$$

Structures fulfilling this conditions have the load such small that it will not come to loss of the stability.

Solution of the stability would look like this:

$$\frac{\chi N_{Ed}}{N_{Rd}} + \frac{\chi_{LT} M_{Ed}}{M_{Rd}} \leq 1.0$$

Therefore, if the calculation is done according to first order theory, second order effects are covered in buckling coefficients χ and χ_{LT} .

2. Second order effects may be calculated by using an analysis appropriate to the structure (including step-by-step or other iterative procedures). For frames where the first sway buckling mode is predominant first order elastic analysis should be carried out with subsequent amplification of relevant action effects (e.g. bending moments) by appropriate factors. This factor can be assumed to be a stability number:

$$\frac{1}{1 - 1/\alpha_{cr}}$$

In this way of calculation buckling coefficients are still used, but in this case, are these coefficients applied on enlarged values of internal forces.

This way of calculation is proposed for the $\alpha_{cr} \geq 3$. For other cases, more accurate second order calculation will be suitable.

3. Solution of the structure accounting all second order effects in calculation using design imperfections. This way of solution should cover nonlinear modelling in specific software. Design imperfection should contain manufacturing and residual stress imperfections. There are some simplifications of these imperfections in Eurocode 3. However, this simplification can be used only for the buckling mode of a bow form. See Table 4.4 Initial bow imperfections.

Table 4.4 Initial bow imperfections

Buckling Curve	Elastic Analysis	Plastic Analysis
	E_0/L	E_0/L
<i>a</i>₀	1/350	1/300
<i>a</i>	1/300	1/250
<i>b</i>	1/250	1/200
<i>c</i>	1/200	1/150
<i>d</i>	1/150	1/100

Buckling curves are given for specific cross-sections. Otherwise all imperfection should be correctly determined. In this solution are second order effects covered in non-linear calculation, buckling coefficients are not applied in this case.

4.7. Scia Engineer

4.7.1. Solution of the wall

Because of the significant deformation of the pile wall a special calculation is performed in Scia Engineer. Second order effects will be examined by nonlinear calculation. Frame is modelled in 2D and all members have assigned geometry and stiffness. The structure is supported by elastic supports representing soil by the stiffness of the spring. The stiffness of the spring is calculated by Schmitt's formula. [6] Spring stiffness according to Schmitt

$$k_h = 2.1 \left(\frac{E^{\frac{4}{3}} o e d}{(EI)^{\frac{1}{3}}} \right).$$

Connections between the struts and the cofferdam walls are modelled as hinges. All cross-sections are set that they correspond to plain strain model – per one meter length of the structure. Lateral earth pressure is entered based on values of normal stress obtained on the interface in the PLAXIS analytical model. Furthermore, the structure is calibrated to correspond to the model in PLAXIS – Schmitt soil modulus is a little bit reduced.

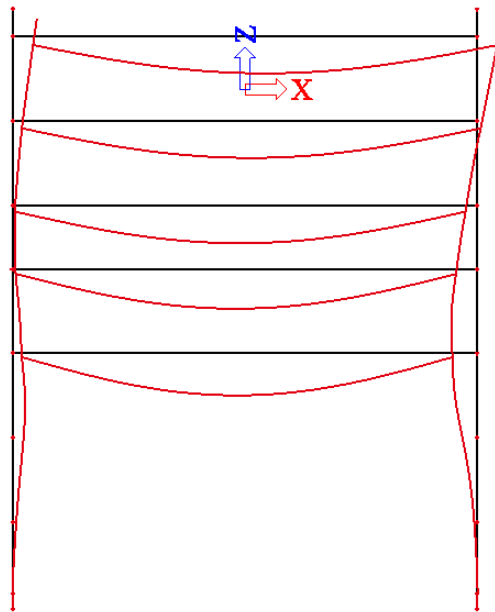


Figure 4.24 Deformed Structure

Loads considered in Scia Engineer

- Self-weight
- Water pressure
- Lateral earth pressure
- Wave load
- Permanent load from the working platform
- Variable load from the working platform

Combinations

Only two combinations are assumed

- CO1 – Linear calculation, responding to Eurocode 7, Design Approach 2
- NC1 – Nonlinear calculation, responding to Eurocode 7, Design Approach 2

Table 4.5 Load cases

Load Case	CO1	NC1
LC1 – Self weight	1,35	1,35
LC2 – Water	1,35	1,35
LC3- Lateral Earth Pressure	1,35	1,35
LC4 -Platform - variable load	1,5	1,5
LC5 - Waves	1,5	1,5
LC6 – Platform -dead load	1,35	1,35

Linear Analysis

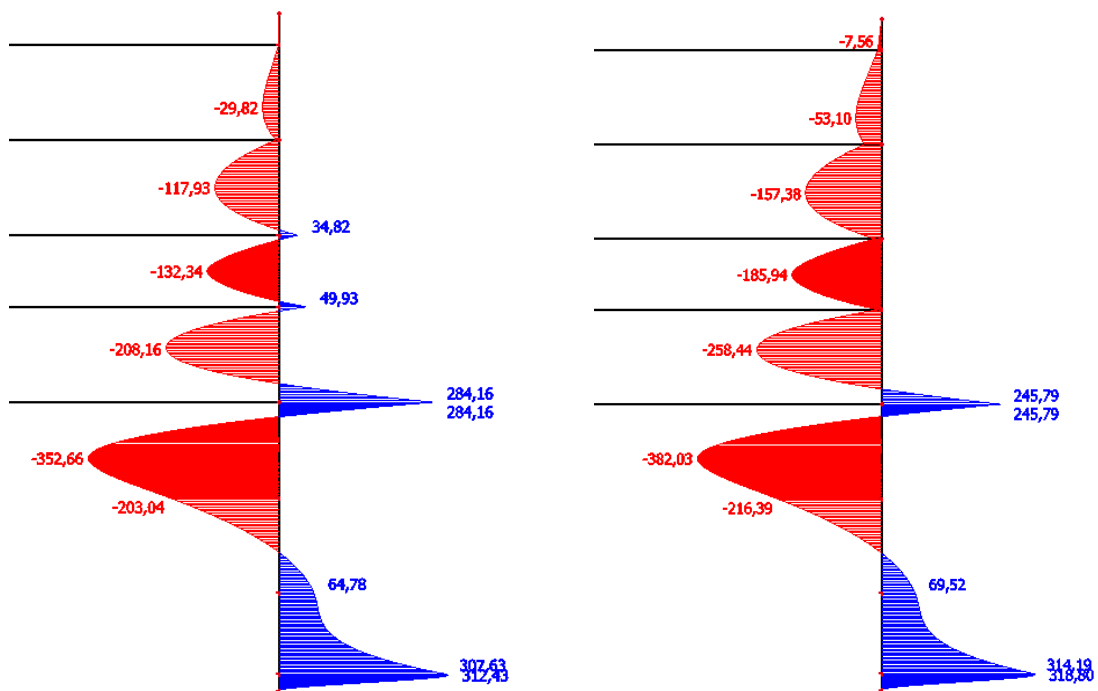
Linear analysis is calibrated to correspond with PLAXIS results. Maximum deformation reached within linear analysis is 31.2 mm where phase displacement in PLAXIS was 31.1 m. In comparison of axial forces, we can see slight difference that is caused by accounted friction in PLAXIS. Forces and bending moments acting in horizontal struts also correspond to values from PLAXIS. If I look at shear forces acting on the wall, I can see no significant difference, however if we compare bending moments we can only see values that are almost five time less than values obtained in PLAXIS. It is not surprising that these values correspond more to results from GEO5. This is caused by the fact that PLAXIS

remembers the bending moment from previous phases, so called influence of locked in stress from previous phases is contained in the results. Where in Scia Engineer the structure is modelled so that we get only the increment. Because obtained values are so small they will not be considered in the design assessment. Even though it was not possible to calibrate bending moments in Scia Engineer with PLAXIS, non-linear calculation was executed in order to observe the change in bending moments.

Non-linear analysis

Non-linear calculation settings

- Global imperfection of the structure is taken from load cases LC2 and LC3
- Picard and Newton-Rapson method is used for the calculation



Linear Bending Moments

Non-linear Bending Moments

Figure 4.25 Bending Moment Diagrams

Maximum bending moment value raised by 10% in non-linear calculation. This value will be compared with the stability and higher value will be considered in the assessment.

Because it was not possible to simulate structure in Scia Engineer as I expected, I decided to try another way of calculating the second order by software. I tried to update mesh in

PLAXIS model after each phase. Even though deformation raised, there was no difference in internal forces.

4.7.2. Horizontal frame

For solution of horizontal frame half of the cofferdam's groundplan is modelled representing symmetry boundary conditions. The waler beam is vertically supported and all struts are connected by hinges. For the solution only one permanent load is applied acting horizontally all around the cofferdam. The value 647 kN/m is characteristic value taken from PLAXIS. It is maximum value that was reached in horizontal struts that were redistributed onto 1 m width of the structure.

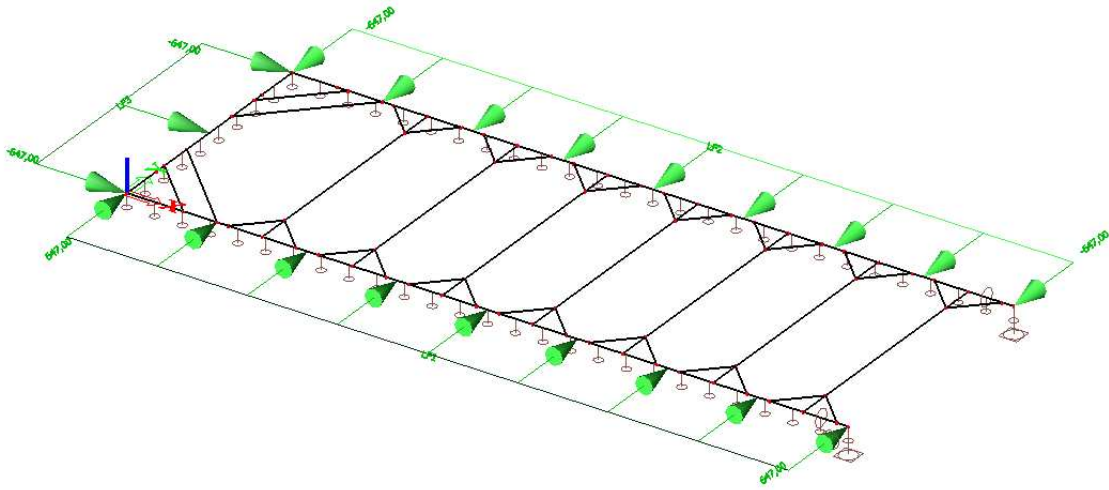


Figure 4.26 Horizontal Frame – Load

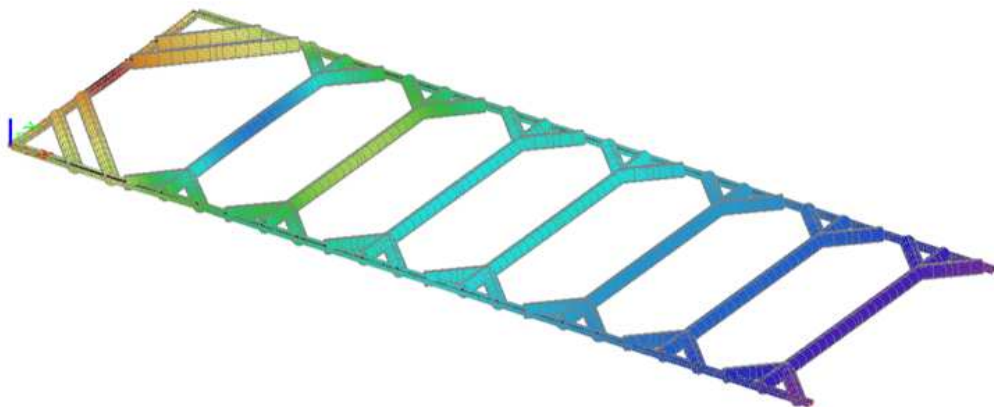


Figure 4.27 Horizontal Frame Deformation

Three combination will be checked in the design of the waler beam. First combination of maximum bending moment and corresponding shear and axial force. Design bending moment of the waler beam reached maximum value of 3909.84 kNm . Corresponding axial force is 9607.95 kN and corresponding shear force 2065.33 kN .

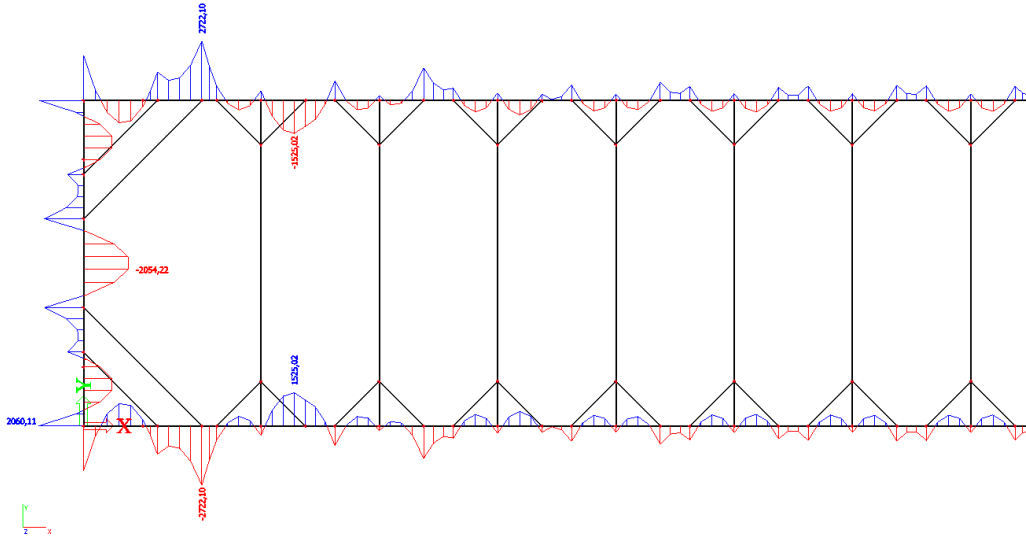


Figure 4.28 Waler Beam Bending Moments

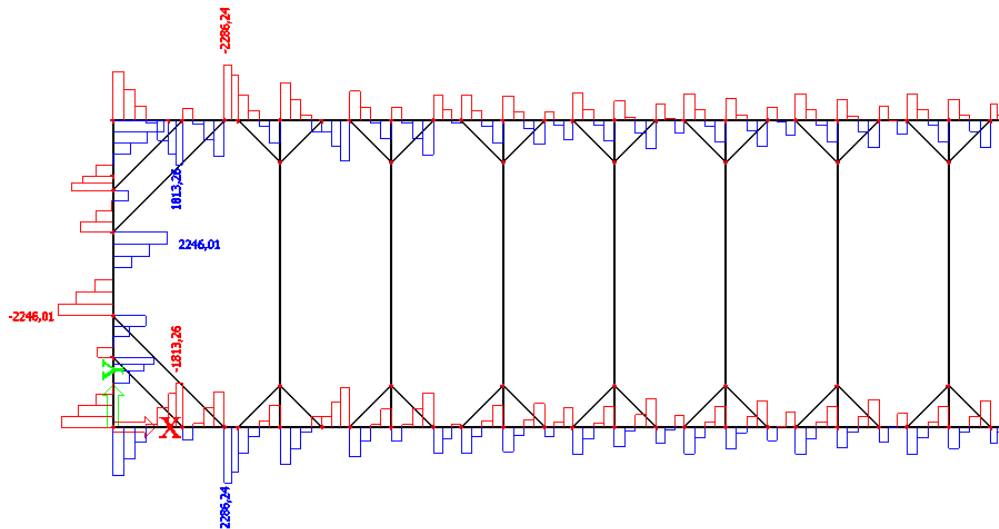


Figure 4.29 Waler Beam Shear Force

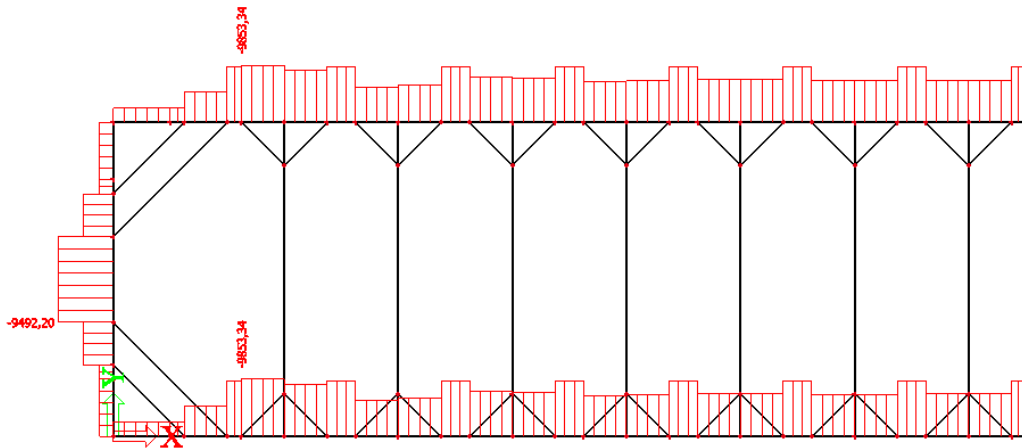


Figure 4.30 Waler Beam Axial Force

Second combination will cover maximum shear force and the last combination will check maximum axial force and corresponding bending moment. In this case values of acting forces are the same as in combination for maximum bending moment.

Another member that will be checked is strut. The most loaded strut is chosen from the horizontal frame and is assessed for maximum design axial load.

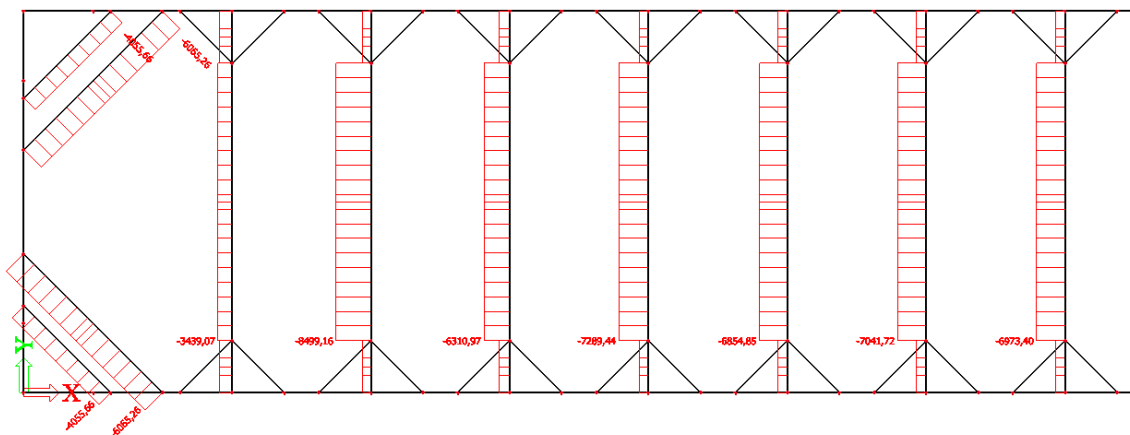


Figure 4.31 Axial Load in Struts

Maximum design axial load is 8160 kN. Additional load from temperature will be assumed for the member assessment.

5. STRUCTURAL ANALYSIS

5.1. Interlocking Pipe Pile Wall

In the preliminary design cross-section of interlocking pipe pile wall was selected with the diameter of 700 mm and wall thickness 16 mm.

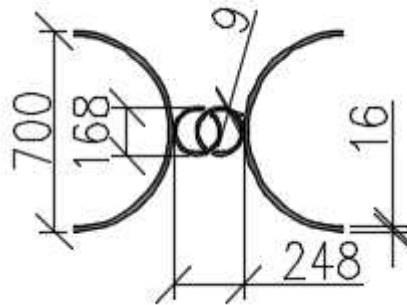


Figure 5.1 Interlocking Pipe Pile Wall 700/16 mm

5.1.1. Material Properties

Structural steel	S355
f_y	355 MPa
E	210 GPa

In case that the design of pipe pile wall 700/16 mm would not be sufficient it is possible to fill the pipes with concrete and increase its bearing capacity.³

5.1.2. Cross-sectional properties

Sectional area..... A	0.0456 m ²
Section modulus..... W	6.07×10 ⁻³ m ³
Shear area..... A_v	0.0290 m ²
Moment of inertia..... I	2.12×10 ⁻³ m ⁴

³ In that case, cross-section would be assessed according to Eurocode 4 - Design of composite steel and concrete structures.

5.1.3. Classification of the cross-section

For tubular cross-sections following rules apply

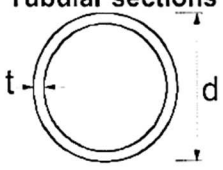
Tubular sections						
						
Class	Section in bending and/or compression					
1	$d/t \leq 50\varepsilon^2$					
2	$d/t \leq 70\varepsilon^2$					
3	$d/t \leq 90\varepsilon^2$					
NOTE For $d/t > 90\varepsilon^2$ see EN 1993-1-6.						
$\varepsilon = \sqrt{235/f_y}$	f_y	235	275	355	420	460
	ε	1,00	0,92	0,81	0,75	0,71
	ε^2	1,00	0,85	0,66	0,56	0,51

Figure 5.2 Tubular Section Classification [9]

For our cross-section

$$\frac{d}{t} = \frac{700}{16} = 43.75 \leq 70\varepsilon^2 = 46.2 \rightarrow \text{class 2}$$

Class 2 cross-sections are those which can develop their plastic moment resistance, but have limited rotation capacity because of local buckling.

5.1.4. Structural Assessment

Structure is loaded by bending moment axial force and shear force. Maximum shear force does not act at the same place as maximum bending moment therefore the structure is assessed for each action separately and finally for interaction of compression and bending moment. Only ultimate limit state is solved.

Maximum Bending Moment

$$M_{Ed} = 1\,406 \text{ kNm/m}$$

Bearing capacity of the cross-section

$$M_{c,Rd} = \frac{W_{pl}f_y}{\gamma_{M0}} = \frac{7.91 \times 10^{-3} 355 \times 10^6}{1.0} = 2\,808 \text{ kNm/m}$$

Second order effects allowance

$$\alpha_{cr} = \frac{N_{cr}}{N_{Ed}} = \frac{30\,514}{1\,209} = 20.25$$

Even though α_{cr} fulfils criteria for first order analysis, second order bending moments influenced by stability number will be determined. First order bending moment is multiplied by stability number to derive second order bending moment.

$$M_{Ed}^{2nd} = \frac{1}{1 - \alpha_{cr}} M_{Ed} = \frac{1}{1 - 1/20.25} 1\,406 = 1\,465 \text{ kNm/m}$$

From non-linear analysis in Scia Engineer 10% change in bending moments was observed. Second order bending moment enlarged by 10% is as follow

$$M_{Ed}^{2nd} = 1.1 M_{Ed} = 1.1 \times 1\,406 = 1\,546 \text{ kNm/m}$$

Bending moment assessment

$$\frac{M_{Ed}}{M_{c,Rd}} \leq 1.0 \dots\dots\dots \frac{1\,406 \text{ kNm/m}}{2\,808 \text{ kNm/m}} = \mathbf{0.50} \leq \mathbf{1.0} \dots\dots\dots \mathbf{\text{cross-section passes}}$$

$$\frac{M_{Ed}^{2nd}}{M_{c,Rd}} \leq 1.0 \dots\dots\dots \frac{1\,546 \text{ kNm/m}}{2\,808 \text{ kNm/m}} = \mathbf{0.55} \leq \mathbf{1.0} \dots\dots\dots \mathbf{\text{cross-section passes}}$$

Maximum axial force

$$N_{Ed} = 1209 \text{ kN/m}$$

Bearing capacity of the cross-section

$$N_{c,Rd} = \frac{A f_y}{\gamma_{M0}} = \frac{45.6 \times 10^{-3} \times 355 \times 10^6}{1.0} = 16\,188 \text{ kN/m}$$

Buckling bearing capacity of the cross-section

In axial compression is buckling bearing capacity multiplied by χ which corresponds to relative slenderness λ . First is necessary to define buckling curve of the cross-section, for rolled hollow sections buckling curve *a* is recommended.

$$N_{b,Rd} = \frac{\chi A f_y}{\gamma_{M0}}$$

$$\chi = \frac{1}{\phi + \sqrt{\phi^2 - \lambda^2}}$$

Where..... $\phi = 0.5[1 + \alpha(\lambda - 0.2) + \lambda^2]$

$\lambda = \sqrt{\frac{Af_y}{N_{cr}}}$ relative slenderness

$N_{cr} = \pi^2 \frac{EI}{L_{cr}^2}$ Euler critical axial force

L_{cr} critical length

α 0.21 for buckling curve a

Estimated critical length is 12 m, it is the longest possible distance between points of the wall securing the position. This length is taken as a conservative value because also the part where soil is resisting the movement of the wall is considered.

Substitution into the formulas

$$N_{cr} = \pi^2 \frac{2.12 \times 10^{-3} 210 \times 10^9}{12^2} = 30\,514 \text{ kN/m}$$

$$\lambda = \sqrt{\frac{45.6 \times 10^{-3} 355 \times 10^6}{30\,514 \times 10^3}} = 0.728$$

$$\phi = 0.5[1 + 0.21(0.728 - 0.2) + 0.728^2] = 0.821$$

$$\chi = \frac{1}{0.821 + \sqrt{0.821^2 - 0.728^2}} = 0.834$$

$$N_{b,Rd} = \frac{\chi Af_y}{\gamma_{M0}} = \frac{0.834 \times 45.6 \times 10^{-3} 355 \times 10^6}{1.0} = 13\,501 \text{ kN/m}$$

Axial force assessment

$$\frac{N_{Ed}}{N_{c,Rd}} \leq 1.0 \dots\dots\dots \frac{1209 \text{ kN/m}}{16188 \text{ kN/m}} = \mathbf{0.07} \leq \mathbf{1.0} \dots\dots\dots \mathbf{\text{cross-section passes}}$$

$$\frac{N_{Ed}}{N_{b,Rd}} \leq 1.0 \dots\dots\dots \frac{1209 \text{ kN/m}}{13\,501 \text{ kN/m}} = \mathbf{0.09} \leq \mathbf{1.0} \dots\dots\dots \mathbf{\text{cross-section passes}}$$

Maximum shear force

$$V_{Ed} = 3364.2 \text{ kN/m}$$

Bearing capacity of the cross-section

$$V_{pl,Rd} = \frac{A_v(f_y/\sqrt{3})}{\gamma_{M0}} = \frac{29 \times 10^{-3} (355 \times 10^6 / \sqrt{3})}{1.0} = 5\,949 \text{ kN/m}$$

Shear force assessment

$$\frac{V_{Ed}}{V_{pl,Rd}} \leq 1.0 \dots\dots\dots \frac{3\,364.2 \text{ kN/m}}{5\,949 \text{ kN/m}} = \mathbf{0.57} \leq \mathbf{1.0} \dots\dots\dots \mathbf{\text{cross-section passes}}$$

Axial compression and bending interaction

Because the cross-section is loaded by axial compression and bending, interaction of these two actions must be verified.

$$\frac{N_{Ed}}{\chi_y N_{Rk}} + k_{yy} \frac{M_{y,Ed}}{\chi_{LT} M_{y,Rk}} + k_{yz} \frac{M_{z,Ed}}{\chi_{LT} M_{z,Rk}} \leq 1$$

$$\frac{N_{Ed}}{\chi_z N_{Rk}} + k_{zy} \frac{M_{y,Ed}}{\chi_{LT} M_{y,Rk}} + k_{zz} \frac{M_{z,Ed}}{\chi_{LT} M_{z,Rk}} \leq 1$$


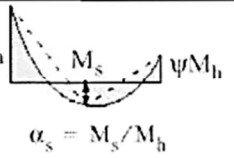
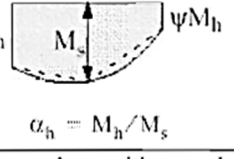
In case of interlocking pipe pile wall, we have no bending moment in plane $z - M_{Ed,z}$, therefore third member of the equation is equal to zero. Also, interaction factors of the wall $k_{yz} = k_{zy} = k_{zz} = 0$.

Determination of interaction factor is done according to Eurocode 3 – simplified method.

Interaction factors	Type of sections	Design assumptions	
		elastic cross-sectional properties class 3, class 4	plastic cross-sectional properties class 1, class 2
k_{yy}	I-sections RHS-sections	$C_{my} \left(1 + 0,6 \bar{\lambda}_y \frac{N_{Ed}}{\chi_y N_{Rk} / \gamma_{M1}} \right)$ $\leq C_{my} \left(1 + 0,6 \frac{N_{Ed}}{\chi_y N_{Rk} / \gamma_{M1}} \right)$	$C_{my} \left(1 + (\bar{\lambda}_y - 0,2) \frac{N_{Ed}}{\chi_y N_{Rk} / \gamma_{M1}} \right)$ $\leq C_{my} \left(1 + 0,8 \frac{N_{Ed}}{\chi_y N_{Rk} / \gamma_{M1}} \right)$
k_{yz}	I-sections RHS-sections	k_{zz}	$0,6 k_{zz}$
k_{zy}	I-sections RHS-sections	$0,8 k_{yy}$	$0,6 k_{yy}$
k_{zz}	I-sections	$C_{mz} \left(1 + 0,6 \bar{\lambda}_z \frac{N_{Ed}}{\chi_z N_{Rk} / \gamma_{M1}} \right)$ $\leq C_{mz} \left(1 + 0,6 \frac{N_{Ed}}{\chi_z N_{Rk} / \gamma_{M1}} \right)$	$C_{mz} \left(1 + (2\bar{\lambda}_z - 0,6) \frac{N_{Ed}}{\chi_z N_{Rk} / \gamma_{M1}} \right)$ $\leq C_{mz} \left(1 + 1,4 \frac{N_{Ed}}{\chi_z N_{Rk} / \gamma_{M1}} \right)$
	RHS-sections		$C_{mz} \left(1 + (\bar{\lambda}_z - 0,2) \frac{N_{Ed}}{\chi_z N_{Rk} / \gamma_{M1}} \right)$ $\leq C_{mz} \left(1 + 0,8 \frac{N_{Ed}}{\chi_z N_{Rk} / \gamma_{M1}} \right)$

For I- and H-sections and rectangular hollow sections under axial compression and uniaxial bending $M_{y,Ed}$ the coefficient k_{zy} may be $k_{zy} = 0$.

Figure 5.3 Interaction factors k_{ij} [9]

Moment diagram	range		C_{my} and C_{mz} and C_{mLT}	
			uniform loading	concentrated load
	$-1 \leq \psi \leq 1$		$0,6 + 0,4\psi \geq 0,4$	
	$0 \leq \alpha_s \leq 1$	$-1 \leq \psi \leq 1$	$0,2 + 0,8\alpha_s \geq 0,4$	$0,2 + 0,8\alpha_s \geq 0,4$
	$-1 \leq \alpha_s < 0$	$0 \leq \psi \leq 1$	$0,1 - 0,8\alpha_s \geq 0,4$	$-0,8\alpha_s \geq 0,4$
$-1 \leq \psi < 0$		$0,1(1-\psi) - 0,8\alpha_s \geq 0,4$	$0,2(-\psi) - 0,8\alpha_s \geq 0,4$	
	$0 \leq \alpha_h \leq 1$	$-1 \leq \psi \leq 1$	$0,95 + 0,05\alpha_h$	$0,90 + 0,10\alpha_h$
	$-1 \leq \alpha_h < 0$	$0 \leq \psi \leq 1$	$0,95 + 0,05\alpha_h$	$0,90 + 0,10\alpha_h$
		$-1 \leq \psi < 0$	$0,95 + 0,05\alpha_h(1+2\psi)$	$\overline{AC2} 0,90 + 0,10\alpha_h(1+2\psi) \overline{AC2}$

For members with sway buckling mode the equivalent uniform moment factor should be taken $C_{my} = 0,9$ or $\overline{AC2} C_{mz} \overline{AC2} = 0,9$ respectively.

C_{my} , C_{mz} and C_{mLT} should be obtained according to the bending moment diagram between the relevant braced points as follows:

moment factor	bending axis	points braced in direction
C_{my}	y-y	z-z
C_{mz}	z-z	y-y
C_{mLT}	y-y	y-y

Figure 5.4 Equivalent Uniform Moment Factors [9]

Table 5.1 Interaction of Bending and Axial force

<i>Cross-section characteristics</i>	
E	210000 MPa
f _y	355 MPa
<i>Material Characteristics</i>	
A	4.56×10 ⁻² m ²
I _y	2.12×10 ⁻³ m ⁴
W _{pl,y}	7.91×10 ⁻³ m ³
<i>Internal forces</i>	
N _{Ed}	1208.25 kN
M _{Ed,y}	1 546 kNm
<i>Buckling</i>	
N _{cr}	30.51 MN
χ _y	0.83
φ _y	0.82
α	0.21 curve a
λ _y	0.73
<i>Cross-sectional resistances</i>	
N _{Rk}	16 188 kN
M _{Rk,y}	2 808 kN
<i>Interaction coefficients</i>	
k _{yy}	1.04
C _{my}	0.99
γ _{M1}	1

$$\frac{1\ 208.25}{\frac{0.83 \times 16\ 188}{1}} + 1.03 \frac{1\ 546}{\frac{2\ 808.05}{1}} = 0.65 \leq 1$$

Cross-section passes

$$\frac{1\ 208.25}{\frac{16\ 188}{1}} = 0.09 \leq 1$$

Cross-section passes

The designed interlocking pipe pile wall $700/_{16}$ mm is sufficient for the structure design.

5.2. Waler Beam

In the preliminary design cross-section of waler beam was selected in a shape of PI chamber after solution in software dimensions are enlarged to dimensions of 900 mm times 900 mm because of the high load.

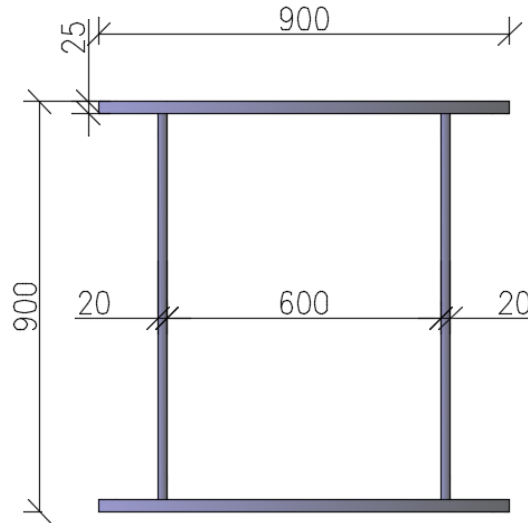


Figure 5.5 Waler beam 900x900 mm

5.2.1. Material Properties

Structural steel	S355
f_y	355 MPa
E	210 GPa

5.2.2. Cross-sectional properties

Sectional area..... A	$8.10 \times 10^{-2} m^2$
Section modulus..... W_{pl}	$2.89 \times 10^{-2} m^3$
Shear area..... A_v	$0.036 m^2$
Moment of inertia..... I	$1.206 \times 10^{-2} m^4$

5.2.3. Classification of the cross-section

The PI chamber cross-section according to Eurocode

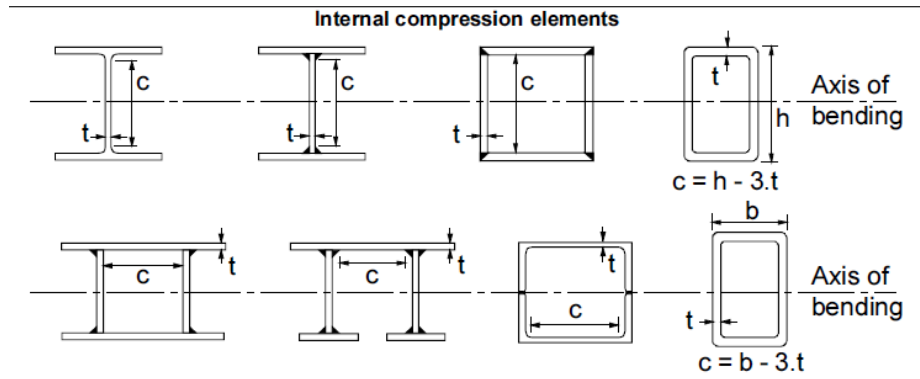


Figure 5.6 Chamber cross-section classification [9]

$$\frac{c}{t} \leq 33\varepsilon \quad \frac{600}{25} = 24 \leq 33 \times 0.81 = 26.73 \quad \text{class 1}$$

Class 1 cross-section are those which can form a plastic hinge with the rotation capacity required for plastic hinges.

5.2.4. Structural Assessment – Ultimate limit state

Waler beam is loaded by combination of bending moment, shear and axial force at a critical section, therefore interaction of all these actions must be considered.

$$M_{Ed,y} = 3\,909.84 \text{ kNm} \quad V_{Ed,z} = 2\,065.33 \text{ kN} \quad N_{Ed} = 9\,607.95 \text{ kN}$$

Independent bearing capacities of the cross-section

$$N_{c,Rd} = \frac{Af_y}{\gamma_{M0}} = \frac{8.10 \times 10^{-2} \times 355 \times 10^6}{1.0} = 28\,755.0 \text{ kN}$$

$$V_{pl,Rd} = \frac{A_v(f_y/\sqrt{3})}{\gamma_{M0}} = \frac{3.60 \times 10^{-2} (355 \times 10^6 / \sqrt{3})}{1.0} = 7\,408.26 \text{ kN}$$

$$M_{c,Rd} = \frac{W_{pl}f_y}{\gamma_{M0}} = \frac{2.08 \times 10^{-2} \times 355 \times 10^6}{1.0} = 10\,263.76 \text{ kNm}$$

Assessment

$$\frac{N_{Ed}}{N_{c,Rd}} \leq 1.0 \dots \frac{9\,607.95 \text{ kN}}{28\,755.0 \text{ kN}} = 0.33 \leq 1.0 \dots \text{cross-section passes}$$

$$\frac{V_{Ed}}{V_{pl,Rd}} \leq 1.0 \dots \frac{2\,065.33 \text{ kN}}{7\,408.26 \text{ kN}} = 0.28 \leq 1.0 \dots \text{cross-section passes}$$

$$\frac{M_{Ed}}{M_{c,Rd}} \leq 1.0 \dots \frac{3\,909.84 \text{ kNm}}{10\,263.76 \text{ kNm}} = 0.38 \leq 1.0 \dots \text{cross-section passes}$$

Buckling bearing capacity of the cross-section

Buckling curve of the cross-section, for PI chamber sections buckling curve *c* is recommended.

$$N_{b,Rd} = \frac{\chi A f_y}{\gamma_{M0}}$$

$$\chi = \frac{1}{\phi + \sqrt{\phi^2 - \lambda^2}}$$

Where..... $\phi = 0.5[1 + \alpha(\lambda - 0.2) + \lambda^2]$

$\lambda = \sqrt{\frac{A f_y}{N_{cr}}}$ relative slenderness

$N_{cr} = \pi^2 \frac{EI}{L_{cr}^2}$ critical axial force

L_{cr} critical length

α 0.49 for buckling curve *c*

Estimated critical length is 70% of the strut's spacing which gives us $L_{cr,y} = 5.6 \text{ m}$. Even though the spacing between side struts is less, we should assume that hinges are not perfectly stiff. For the plane *zz* critical length is assumed as length between horizontal struts $L_{cr,y} = 8.0 \text{ m}$, there will be an element securing the position of the waler beam in *z* direction at each strut.

$$N_{cr,y} = \pi^2 \frac{1.21 \times 10^{-2} 210 \times 10^9}{5.6^2} = 796 \text{ MN}$$

$$\lambda_y = \sqrt{\frac{8.1 \times 10^{-2} 355 \times 10^6}{796 \times 10^6}} = 0.190$$

$$\phi_y = 0.5 \times [1 + 0.49 \times (0.19 - 0.2) + 0.19^2] \\ = 0.516$$

$$\chi_y = \frac{1}{0.516 + \sqrt{0.516^2 - 0.19^2}} = 1.0$$

$$N_{cr,z} = \pi^2 \frac{6.50 \times 10^{-3} 210 \times 10^9}{8.0^2} = 210 \text{ MN}$$

$$\lambda_z = \sqrt{\frac{8.1 \times 10^{-2} 355 \times 10^6}{210 \times 10^6}} = 0.370$$

$$\phi_z = 0.5 \times [1 + 0.49 \times (0.37 - 0.2) + 0.37^2] \\ = 0.610$$

$$\chi_z = \frac{1}{0.61 + \sqrt{0.61^2 - 0.37^2}} = 0.91$$

$$N_{b,Rd,y} = \frac{\chi A f_y}{\gamma_{M0}} = \frac{1 \times 8.1 \times 10^{-2} \times 355 \times 10^6}{1.0} = 28\,755.0 \text{ kN}$$

$$N_{b,Rd,z} = \frac{\chi A f_y}{\gamma_{M0}} = \frac{0.91 \times 8.1 \times 10^{-2} \times 355 \times 10^6}{1.0} = 26\,260 \text{ kN}$$

Axial force assessment

$$\frac{N_{Ed}}{N_{b,Rd,z}} \leq 1.0 \dots\dots\dots \frac{9\,607 \text{ kN}}{26\,260 \text{ kN}} = \mathbf{0.37} \leq \mathbf{1.0} \dots\dots\dots \mathbf{\text{cross-section passes}}$$

Interaction of shear force bending moment and axial force assessment

Because of high values of all three internal forces, bending moment capacity should be reduced according to Eurocode 3. Shear force allowance can be neglected if

$$V_{Ed} \leq 0.5 V_{pl,Rd}$$

$$2\,065.33 \text{ kN} \leq 3\,704.26 \text{ kN}$$

As far as this condition is fulfilled, shear force effect on bending moment bearing capacity must not be considered. For double symmetrical section with flanges, allowance need not be made for the effect of the axial force on plastic resistance moment about the y-y axis when both the following criteria are satisfied [9]

$$N_{Ed} \leq 0.25 N_{pl,Rd}$$

$$9\,607.95 \text{ kN} \not\leq 7\,188.75 \text{ kN}$$

$$N_{Ed} \leq \frac{0.5 h_w t_w f_y}{\gamma_{M0}}$$

Already the first condition is not satisfied, therefore effect of axial force must be considered. For class 1 and 2 cross sections, the following criteria shall be satisfied

$$M_{Ed} \leq M_{N,Rd}$$

where $M_{N,Rd}$ is reduced design value of the bending moment resistance, making allowance for the presence of normal forces.

$$M_{N,Rd} = M_{pl,Rd} (1 - n) / (1 - 0.5 a_w) \quad \text{but} \quad M_{N,Rd} \leq M_{pl,Rd}$$

Where

$$n = \frac{N_{Ed}}{N_{pl,Rd}} \quad \text{but} \quad a_w \leq 0.5$$

$$a_w = \frac{A - 2bt}{A}$$

$$n = \frac{9\,607.95 \text{ kN}}{28\,755 \text{ kN}} = 0.33$$

$$a_w = \frac{8.1 \times 10^{-2} - 2 \times 0.9 \times 0.025}{8.1 \times 10^{-2}} = 0.44$$

Reduced bending moment assessment

$$M_{N,Rd} = 10\,263.76 \times \frac{(1-0.33)}{(1-0.5 \times 0.44)} = 8\,786.97 \text{ kNm} \dots \leq 10\,263.76 \text{ kNm}$$

$$M_{Ed} \leq M_{N,Rd} \dots \mathbf{3\,909.84 \text{ kNm} \leq 8\,786.97 \text{ kNm}} \dots \mathbf{\text{cross-section passes}}$$

Interaction of axial compression and bending assessment

In case of normal force acting, also interaction of compression and bending moment must be considered. The equations are the same as shown in calculation of the wall.

$$\frac{N_{Ed}}{\frac{\chi_y N_{Rk}}{\gamma_{M1}}} + k_{yy} \frac{M_{y,Ed}}{\frac{\chi_{LT} M_{y,Rk}}{\gamma_{M1}}} + k_{yz} \frac{M_{z,Ed}}{\frac{\chi_{LT} M_{z,Rk}}{\gamma_{M1}}} \leq 1$$

$$\frac{N_{Ed}}{\frac{\chi_z N_{Rk}}{\gamma_{M1}}} + k_{zy} \frac{M_{y,Ed}}{\frac{\chi_{LT} M_{y,Rk}}{\gamma_{M1}}} + k_{zz} \frac{M_{z,Ed}}{\frac{\chi_{LT} M_{z,Rk}}{\gamma_{M1}}} \leq 1$$

Cross-section characteristics	
E	210000 MPa
f _y	355 MPa
Material Characteristics	
A	8.10×10 ⁻² m ²
I _y	1.21×10 ⁻² m ⁴
I _z	6.50×10 ⁻³ m ⁴
W _{pl,y}	2.89×10 ⁻² m ³
W _{pl,z}	2.13×10 ⁻² m ³
Internal forces	
N _{Ed}	9607.95 kN
M _{Ed,y}	3909.84 kNm
M _{Ed,z}	0.00 kNm
Cross-sectional resistances	
N _{Rk}	28 755.00 kN
M _{Rk,y}	10 263.76 kN
Interaction coefficients	
k _{yy}	0.96
k _{zy}	0.57
C _{my}	0.96
C _{my}	0.96
γ _{M1}	1

$$\frac{9\,607.95}{\frac{1 \times 28\,755}{1}} + 0.96 \frac{3\,909.84}{\frac{10\,263.76}{1}} = 0.70 \leq 1$$

Cross-section passes

$$\frac{9\,607.95}{\frac{0.91 \times 28\,755}{1}} + 0.57 \frac{3\,909.84}{\frac{10\,263.76}{1}} = 0.69 \leq 1$$

Cross-section passes

5.2.5. Check against disproportionate collapse

If we assume that the most loaded strut collapses. Waling beam must be checked for the case of single strut collapse.

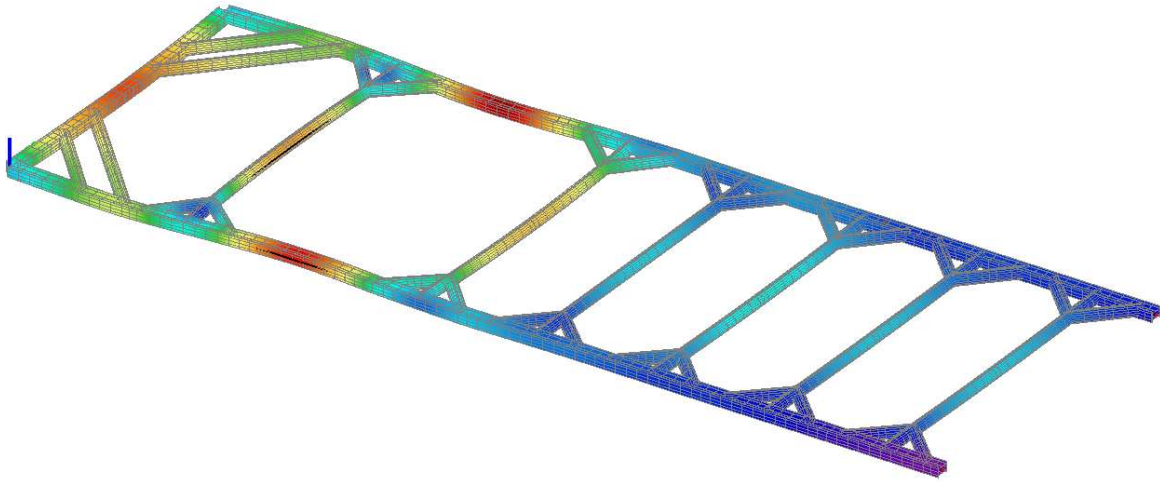


Figure 5.7 Structure without originally most loaded strut

For the assessment of disproportionate collapse characteristic combination is assumed.

Maximum internal forces acting on waling beam

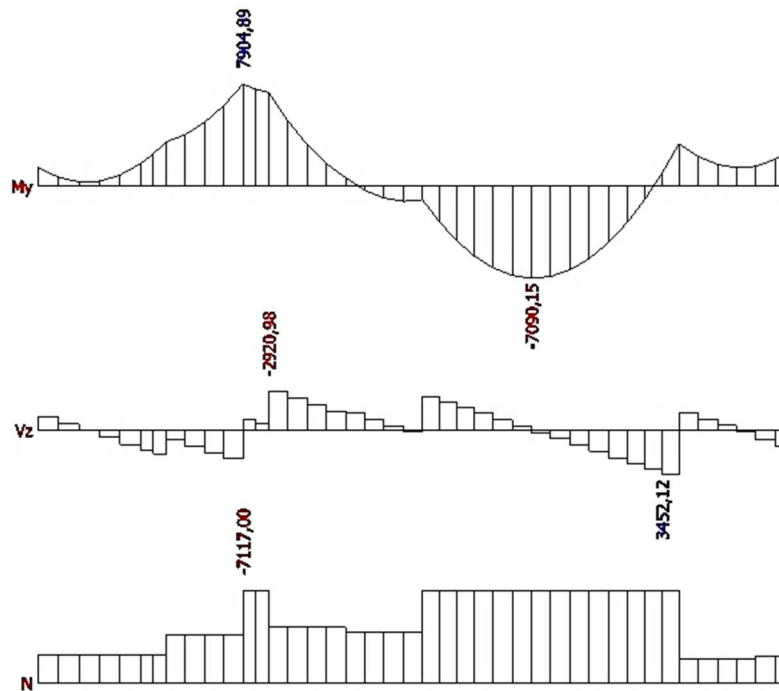


Figure 5.8 Internal forces

In this case, maximum shear force is not at the same place as maximum bending moment. Therefore, two combinations will be assessed.

Combination for maximum bending moment

$$M_{Ed,y} = 7\,904.89 \text{ kNm}$$

$$V_{Ed,z} = 2\,216 \text{ kN}$$

$$N_{Ed} = 7\,117 \text{ kN}$$

Independent capacities assessment

$$\frac{N_{Ed}}{N_{c,Rd}} \leq 1.0 \dots\dots\dots \frac{7\,117 \text{ kN}}{28\,755.0 \text{ kN}} = \mathbf{0.24} \leq \mathbf{1.0} \dots\dots\dots \mathbf{\text{cross-section passes}}$$

$$\frac{V_{Ed}}{V_{pl,Rd}} \leq 1.0 \dots\dots\dots \frac{2\,216 \text{ kN}}{7\,408.26 \text{ kN}} = \mathbf{0.30} \leq \mathbf{1.0} \dots\dots\dots \mathbf{\text{cross-section passes}}$$

$$\frac{M_{Ed}}{M_{c,Rd}} \leq 1.0 \dots\dots\dots \frac{7\,904.89 \text{ kNm}}{10\,263.76 \text{ kNm}} = \mathbf{0.76} \leq \mathbf{1.0} \dots\dots\dots \mathbf{\text{cross-section passes}}$$

$$\frac{N_{Ed}}{N_{b,Rd,z}} \leq 1.0 \dots\dots\dots \frac{7\,117 \text{ kN}}{26\,260 \text{ kN}} = \mathbf{0.27} \leq \mathbf{1.0} \dots\dots\dots \mathbf{\text{cross-section passes}}$$

Interaction of shear force bending moment and axial force assessment

Shear force allowance can be neglected if

$$V_{Ed} \leq 0.5 V_{pl,Rd}$$

$$2\,216 \text{ kN} \leq 3\,704.16 \text{ kN}$$

As far as this condition is fulfilled, shear force effect on bending moment bearing capacity must not be considered. Allowance need not be made for the effect of the axial force on plastic resistance moment about the y-y axis when both the following criteria are satisfied [9]

$$N_{Ed} \leq 0.25 N_{pl,Rd}$$

$$7\,117 \text{ kN} \leq 7\,188.75 \text{ kN}$$

$$N_{Ed} \leq \frac{0.5 h_w t_w f_y}{\gamma_{M0}}$$

$$7\,117 \text{ kN} \not\leq \frac{0.5 \times 0.85 \times 0.04 \times 355 \times 10^3}{1} = 6\,035 \text{ kN}$$

As far as the second condition is not satisfied, effect of axial force must be considered. For class 1 and 2 cross sections, the following criteria shall be satisfied

$$M_{Ed} \leq M_{N,Rd}$$

where $M_{N,Rd}$ is reduced design value of the bending moment resistance, making allowance for the presence of normal forces.

$$M_{N,Rd} = M_{pl,Rd}(1 - n)/(1 - 0.5a_w) \quad \text{but} \quad M_{N,Rd} \leq M_{pl,Rd}$$

Where

$$n = \frac{N_{Ed}}{N_{pl,Rd}}$$

$$a_w = \frac{A - 2bt}{A} \quad \text{but} \quad a_w \leq 0.5$$

$$n = \frac{7\,117\text{ kN}}{28\,755\text{ kN}} = 0.25$$

$$a_w = \frac{8.1 \times 10^{-2} - 2 \times 0.9 \times 0.025}{8.1 \times 10^{-2}} = 0.44$$

Reduced bending moment assessment

$$M_{N,Rd} = 10\,263.76 \times \frac{(1-0.25)}{(1-0.5 \times 0.44)} = 9\,930.12\text{ kNm} \leq 10\,263.76\text{ kNm}$$

$$M_{Ed} \leq M_{N,Rd} \dots \dots \dots \mathbf{7\,904.89\text{ kNm} \leq 9\,930.12\text{ kNm} \dots \dots \dots \text{cross-section passes}}$$

Interaction of axial compression and bending assessment

$$\frac{N_{Ed}}{\frac{\chi_y N_{Rk}}{\gamma_{M1}}} + k_{yy} \frac{M_{y,Ed}}{\frac{\chi_{LT} M_{y,Rk}}{\gamma_{M1}}} + k_{yz} \frac{M_{z,Ed}}{\frac{\chi_{LT} M_{z,Rk}}{\gamma_{M1}}} \leq 1$$

$$\frac{N_{Ed}}{\frac{\chi_z N_{Rk}}{\gamma_{M1}}} + k_{zy} \frac{M_{y,Ed}}{\frac{\chi_{LT} M_{y,Rk}}{\gamma_{M1}}} + k_{zz} \frac{M_{z,Ed}}{\frac{\chi_{LT} M_{z,Rk}}{\gamma_{M1}}} \leq 1$$

Cross-section characteristics	
E	210000 MPa
f _y	355 MPa
Material Characteristics	
A	8.10×10 ⁻² m ²
I _y	1.21×10 ⁻² m ⁴
I _z	6.50×10 ⁻³ m ⁴
W _{pl,y}	2.89×10 ⁻² m ³
W _{pl,z}	2.13×10 ⁻² m ³
Internal forces	
N _{Ed}	7 117 kN
M _{Ed,y}	7 841 kNm
M _{Ed,z}	0.00 kNm
Cross-sectional resistances	
N _{Rk}	28 755.00 kN
M _{Rk,y}	10 263.76 kN
Interaction coefficients	
k _{yy}	0.96
k _{zy}	0.57
C _{my}	0.96
C _{my}	0.96
γ _{M1}	1

$$\frac{7\,117}{\frac{1 \times 28\,755}{1}} + 0.96 \frac{7\,904.89}{\frac{10\,263.76}{1}} = 0.99 \leq 1$$

Cross-section passes

$$\frac{7\,117}{\frac{0.91 \times 28\,755}{1}} + 0.57 \frac{7\,904.89}{\frac{10\,263.76}{1}} = 0.69 \leq 1$$

Cross-section passes

Maximum shear force

$$V_{Ed,max} = 3\,491.12 \text{ kN}$$

$$\frac{V_{Ed}}{V_{pl,Rd}} \leq 1.0 \dots\dots\dots \frac{3\,491.12\text{ kN}}{7\,408.26\text{ kN}} = 0.47 \leq 1.0 \dots\dots\dots \text{cross-section passes}$$

The designed water beam of the PI chamber section 900/900 mm is sufficient for the design.

5.3. Horizontal Strut

In the preliminary design cross-section of struts in strut level 4 was selected with the diameter of 1016 mm and wall thickness 32 mm. After solution in the software and checking by hand the dimensions of this strut were reduced to 813/27 mm. As mentioned previously temperature effect on struts is considered in the design. Strut that is maximally loaded is marked in the picture. This strut is simultaneously longest and therefore the only one that will be assessed.

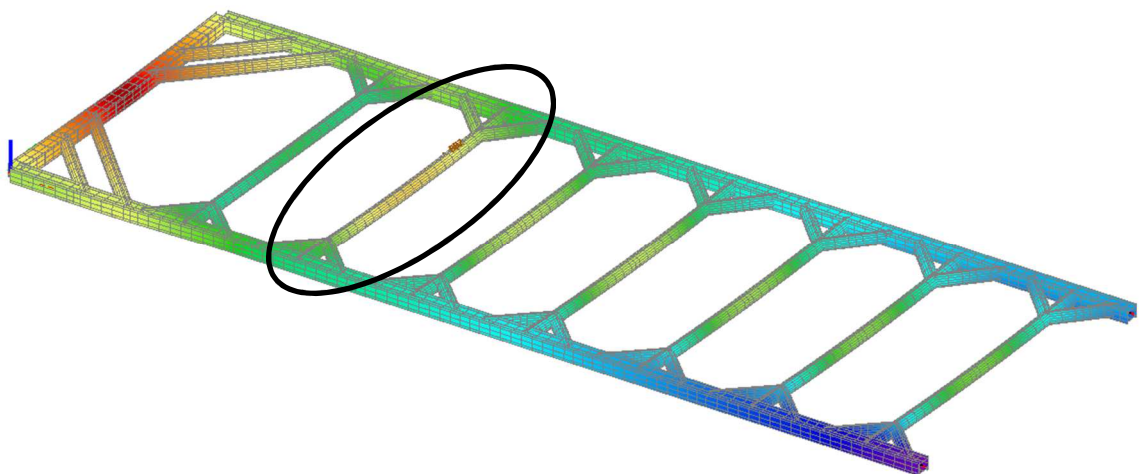


Figure 5.9 Horizontal Frame- maximally loaded strut

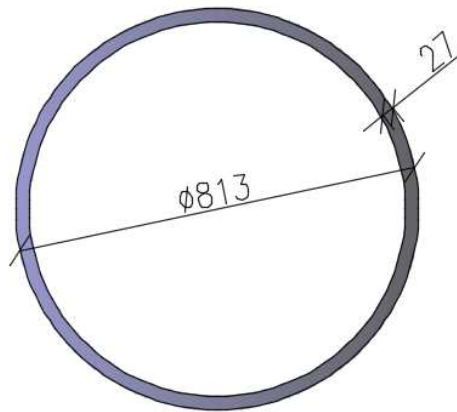


Figure 5.10 Strut Cross-section

5.3.1. Material Properties

Structural steel	S355
f_y	355 MPa
E	210 GPa

5.3.2. Cross-sectional properties

Sectional area..... A	$6.67 \times 10^{-2} m^2$
Section modulus..... W	$1.67 \times 10^{-2} m^3$
Shear area..... A_v	$4.24 \times 10^{-2} m^2$
Moment of inertia..... I	$5.15 \times 10^{-3} m^4$

5.3.3. Classification of the cross-section

For our cross-section CHS 813/27 mm

$$\frac{d}{t} = \frac{813}{27} = 30.11 \leq 50\epsilon^2 = 33.0 \rightarrow \text{class 1}$$

Class 1 cross-section are those which can form a plastic hinge with the rotation capacity required for plastic hinges.

5.3.4. Structural Assessment – Ultimate limit state

Horizontal strut will be checked in two sections – in the middle of the span and in section 3 meters from the end. Because I do not know which of these sections will give worse results, it is necessary to test both.

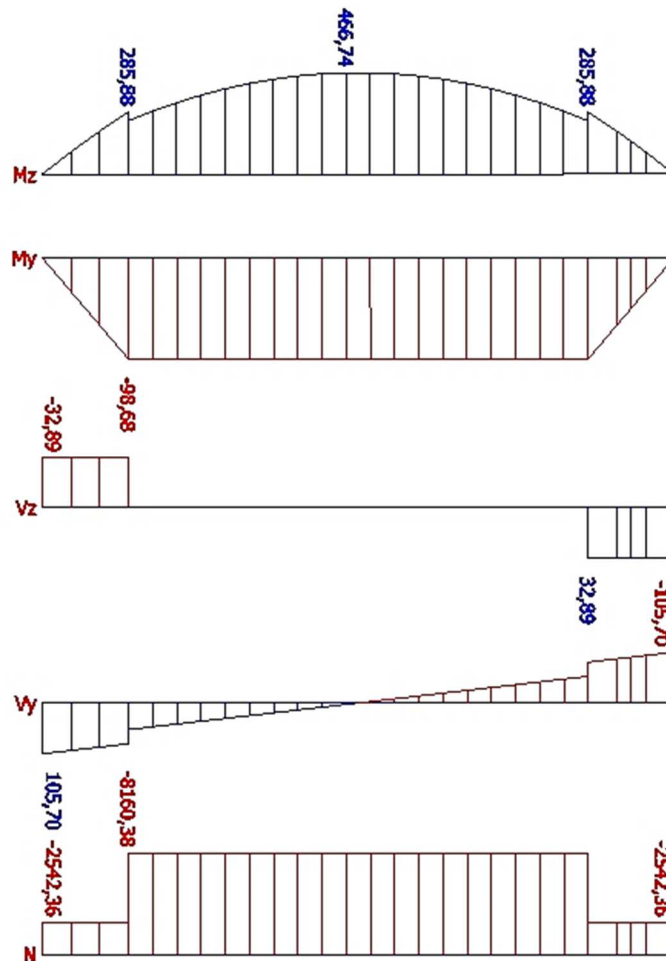


Figure 5.11 Strut - Internal Forces

In chapter temperature load on struts I have discussed the topic of why it is necessary to consider temperature in a design of struts. Positive temperature change ΔT gives us an extra axial load in strut. The magnitude of this load is dependent on the cross-section, length of the strut, level of restraint and other. If the structure is completely restrained, elastic calculation would be applicable.

$$P = \alpha EA \Delta t$$

However, in my case the structure cannot be considered as fully restrained, because it can deflect. The procedure of calculation that was introduced by Chapman et. al. [5] is more suitable for the solution of this horizontal strut.

$$\Delta P = \frac{A_s E_s \alpha \Delta T}{1 + \frac{3n A_s E_s H}{A_w E_{def} L}} \quad [kN]$$

E_s	210	GPa
A_s	6.67×10^{-2}	m^2
A_w	28	m^2
L	22	m
H	18.8	m
α	1.2×10^{-5}	K^{-1}
ΔT	25	$^{\circ}C$
E_{def}	?	MPa

Derivation of deformation modulus is not as clear as for uniform ground. Because there are several layers and the wall is propped only by water in the upper part two ways of modulus determinations were used.

1. Average E_{def}

An average value of deformation modulus along the wall.

$$E_{def} = 13.22 \text{ MPa}$$

$$\Delta P = \frac{6.67 \times 10^{-2} \times 210 \times 10^6 \times 1.2 \times 10^{-5} \times 25}{1 + \frac{3 \times 6.67 \times 10^{-2} \times 210 \times 10^6 \times 18.8}{28 \times 13.22 \times 10^3 \times 22}} = 42.79 \text{ kN}$$

2. E_{def} of ground layer in the depth of the strut S4

$$E_{def} = 8 \text{ MPa}$$

$$\Delta P = \frac{6.67 \times 10^{-2} \times 210 \times 10^6 \times 1.2 \times 10^{-5} \times 25}{1 + \frac{3 \times 6.67 \times 10^{-2} \times 210 \times 10^6 \times 18.8}{28 \times 8 \times 10^3 \times 22}} = 26.01 \text{ kN}$$

We can see that both values are very small. The deflection of a wall reduces significantly axial load evoked by temperature change in the strut. If we examine elastic calculation, which would not correspond to a real structure we will get much greater value.

$$\Delta P = \alpha E A \Delta T = 6.67 \times 10^{-2} \times 210 \times 10^6 \times 1.2 \times 10^{-5} \times 25 = 3924.9 \text{ kN}$$

This value is not realistic for the case of cofferdam therefore value calculated according to Chapman [5] of $\Delta P_d = 1.5 \times 42.79 = 64.19 \text{ kN}$ is assumed in the design.

SECTION 1 – $x = 11 \text{ m}$

$$N_{Ed} = -8\,225 \text{ kN}$$

$$V_{Ed,y} = 0 \text{ kN}$$

$$V_{Ed,z} = 0 \text{ kN}$$

$$M_{Ed,z} = 466.74 \text{ kNm}$$

$$M_{Ed,y} = -98.68 \text{ kNm}$$

SECTION 2 – $x = 3 \text{ m}$

$$N_{Ed} = -8\,225 \text{ kN}$$

$$V_{Ed,y} = 84.89 \text{ kN}$$

$$V_{Ed,z} = -32.88 \text{ kN}$$

$$M_{Ed,z} = 285.88 \text{ kNm}$$

$$M_{Ed,y} = -98.68 \text{ kNm}$$

Single bearing capacities assessment

$$N_{c,Rd} = \frac{A f_y}{\gamma_{M0}} = \frac{6.67 \times 10^{-2} \times 355 \times 10^6}{1.0} = 23\,678 \text{ kN}$$

$$V_{pl,Rd} = \frac{A_v (f_y / \sqrt{3})}{\gamma_{M0}} = \frac{4.24 \times 10^{-2} (355 \times 10^6 / \sqrt{3})}{1.0} = 8\,699.29 \text{ kN}$$

$$M_{c,Rd} = \frac{W_{pl} f_y}{\gamma_{M0}} = \frac{1.67 \times 10^{-2} \times 355 \times 10^6}{1.0} = 5\,928.5 \text{ kNm}$$

Bearing Capacity	Section 1	Section 2	Assessment
$N_{c,Rd} = 23\,678 \text{ kN}$	$N_{Ed} = -8\,225 \text{ kN}$	$N_{Ed} = -8\,225 \text{ kN}$	$0.35 \leq 1$ PASSES
$V_{pl,Rd} = 8\,699.29 \text{ kN}$	$V_{Ed} = 0 \text{ kN}$	$V_{Ed,MAX} = 84.89 \text{ kN}$	$0.01 \leq 1$ PASSES
$M_{c,Rd} = 5\,928.5 \text{ kNm}$	$M_{Ed,max} = 466.74 \text{ kNm}$	$M_{Ed,max} = 285.88 \text{ kNm}$	$0.08 \leq 1$ PASSES

Buckling bearing capacities of the cross-section

Buckling must be solved in the plane of bending and from the plane of bending. Critical length of the strut is assumed as whole length in both directions.

$$N_{cr,y} = N_{cr,z} = \pi^2 \frac{5.15 \times 10^{-3} \times 210 \times 10^9}{22^2} = 22\,073.8 \text{ kN}$$

$$\lambda = \sqrt{\frac{6.67 \times 10^{-2} \times 355 \times 10^6}{22\,073.8 \times 10^3}} = 1.036$$

$$\phi = 0.5[1 + 0.21(1.036 - 0.2) + 1.036^2] = 1.12$$

$$\chi = \frac{1}{1.12 + \sqrt{1.12^2 - 1.036^2}} = 0.64$$

$$N_{b,Rd,y} = N_{b,Rd,z} = \frac{\chi A f_y}{\gamma_{M0}} = \frac{0.64 \times 6.23 \times 10^{-2} \times 355 \times 10^6}{1.0} = 15\,168.62 \text{ kN/m}$$

Buckling assessment

$$\frac{N_{Ed}}{N_{b,Rd}} \leq 1.0 \dots \frac{8\,225 \text{ kN/m}}{15\,168.62 \text{ kN/m}} = \mathbf{0.54} \leq \mathbf{1.0} \dots \text{cross-section passes}$$

Combination of axial compression and bending assessment

Cross-section characteristics	
E	210000 MPa
f _y	355 MPa
Material Characteristics	
A	6.67×10 ⁻² m ²
I _y	5.15×10 ⁻³ m ⁴
I _z	5.15×10 ⁻³ m ⁴
W _{pl,y}	1.67×10 ⁻² m ³
W _{pl,z}	1.67×10 ⁻² m ³
Internal forces - Section 1	
N _{Ed}	8 225 kN
M _{Ed,y}	-98.68 kNm
M _{Ed,z}	466.74 kNm
Internal forces - Section 2	
N _{Ed}	8 225 kN
M _{Ed,y}	-98.68 kNm
M _{Ed,z}	285.88 kNm
Cross-sectional resistances	
N _{Rk}	23 678.50 kN
M _{Rk,y}	5 923.89 kN
Interaction coefficients	
k _{yy}	1.45
k _{zy}	0.87
k _{zz}	1.45
k _{yz}	0.87
C _{my}	1.01
C _{my}	1.01
γ _{M1}	1

$$\frac{N_{Ed}}{\frac{\chi_y N_{Rk}}{\gamma_{M1}}} + k_{yy} \frac{M_{y,Ed}}{\frac{\chi_{LT} M_{y,Rk}}{\gamma_{M1}}} + k_{yz} \frac{M_{z,Ed}}{\frac{\chi_{LT} M_{z,Rk}}{\gamma_{M1}}} \leq 1$$

$$\frac{N_{Ed}}{\frac{\chi_z N_{Rk}}{\gamma_{M1}}} + k_{zy} \frac{M_{y,Ed}}{\frac{\chi_{LT} M_{y,Rk}}{\gamma_{M1}}} + k_{zz} \frac{M_{z,Ed}}{\frac{\chi_{LT} M_{z,Rk}}{\gamma_{M1}}} \leq 1$$

Section 1 ($x = 11 \text{ m}$):

$$\frac{8\,225}{\frac{0.64 \times 23\,678.50}{1}} + 1.45 \frac{98.68}{\frac{5\,923.89}{1}} + 0.87 \frac{466.74}{\frac{5\,923.89}{1}} = 0.63 \leq 1 \quad \text{PASSES}$$

$$\frac{8\,225}{\frac{0.64 \times 23\,678.50}{1}} + 0.87 \frac{98.68}{\frac{5\,923.89}{1}} + 1.45 \frac{466.74}{\frac{5\,923.89}{1}} = 0.67 \leq 1 \quad \text{PASSES}$$

Section 2 ($x = 3 \text{ m}$):

$$\frac{8\,225}{\frac{0.64 \times 23\,678.50}{1}} + 1.45 \frac{98.68}{\frac{5\,923.89}{1}} + 0.87 \frac{285.88}{\frac{5\,923.89}{1}} = 0.61 \leq 1 \quad \text{PASSES}$$

$$\frac{8\,225}{\frac{0.64 \times 23\,678.50}{1}} + 0.87 \frac{98.68}{\frac{5\,923.89}{1}} + 1.45 \frac{285.88}{\frac{5\,923.89}{1}} = 0.63 \leq 1 \quad \text{PASSES}$$

5.3.1. Check against disproportionate collapse

If the most loaded strut collapses redistribution of internal forces is as follow. For the assessment of disproportionate collapse characteristic combination is assumed.

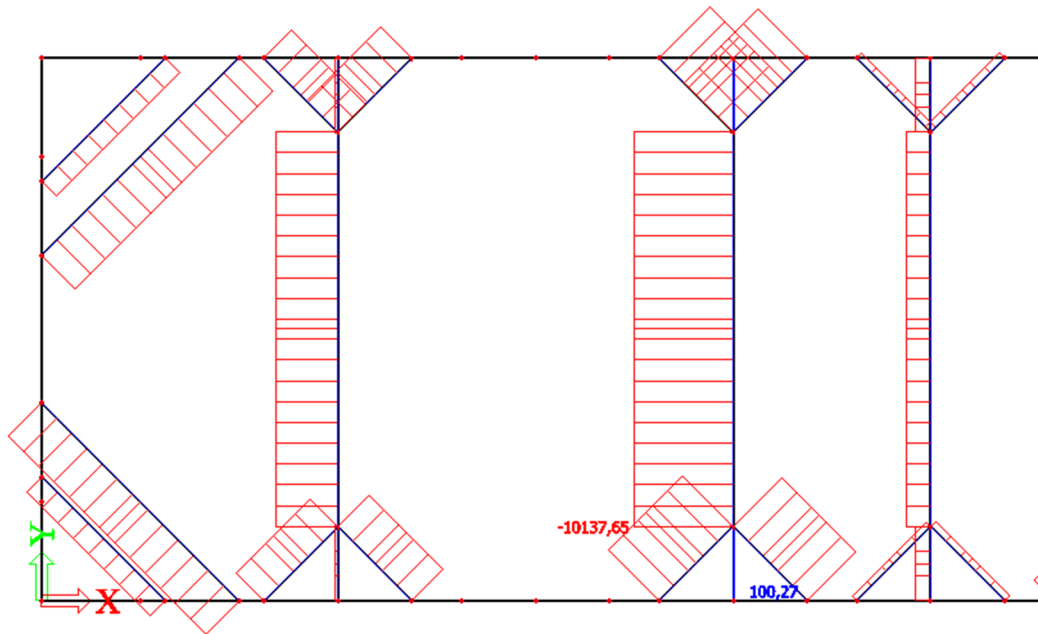


Figure 5.12 Axial Force Redistribution

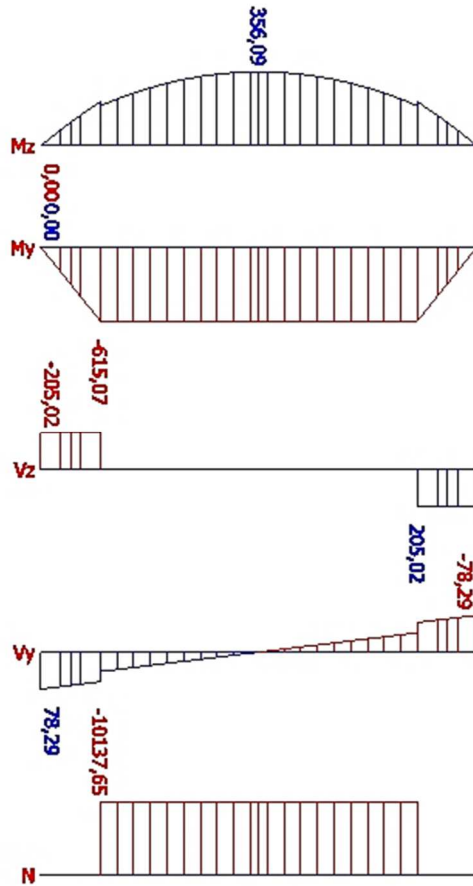


Figure 5.13 Strut - Internal Forces

SECTION 1 – $x = 11 \text{ m}$

$$N_{Ed} = -10\,202 \text{ kN}$$

$$V_{Ed,y} = 0 \text{ kN}$$

$$V_{Ed,z} = 0 \text{ kN}$$

$$M_{Ed,z} = 356.09 \text{ kNm}$$

$$M_{Ed,y} = -615.07 \text{ kNm}$$

SECTION 2 – $x = 3 \text{ m}$

$$N_{Ed} = -10\,202 \text{ kN}$$

$$V_{Ed,y} = 62.88 \text{ kN}$$

$$V_{Ed,z} = -205.02 \text{ kN}$$

$$M_{Ed,z} = 211.77 \text{ kNm}$$

$$M_{Ed,y} = -615.07 \text{ kNm}$$

Single Bearing capacities assessment

$$N_{c,Rd} = \frac{A f_y}{\gamma_{M0}} = \frac{6.67 \times 10^{-2} 355 \times 10^6}{1.0} = 23\,678 \text{ kN}$$

$$V_{pl,Rd} = \frac{A_v (f_y / \sqrt{3})}{\gamma_{M0}} = \frac{4.24 \times 10^{-2} (355 \times 10^6 / \sqrt{3})}{1.0} = 8\,699.29 \text{ kN}$$

$$M_{c,Rd} = \frac{W_{pl} f_y}{\gamma_{M0}} = \frac{1.67 \times 10^{-2} 355 \times 10^6}{1.0} = 5\,928.5 \text{ kNm}$$

Bearing Capacity	Section 1	Section 2	Assessment
$N_{c,Rd} = 23\,678\text{ kN}$	$N_{Ed} = -10\,202\text{ kN}$	$N_{Ed} = -10\,202\text{ kN}$	$0.43 \leq 1$ PASSES
$V_{pl,Rd} = 8\,699.29\text{ kN}$	$V_{Ed} = 0\text{ kN}$	$V_{Ed,MAX} = 205.02\text{ kN}$	$0.02 \leq 1$ PASSES
$M_{c,Rd} = 5\,928.5\text{ kNm}$	$M_{Ed,max} = 615.07\text{ kNm}$	$M_{Ed,max} = 615.07\text{ kNm}$	$0.10 \leq 1$ PASSES

Buckling assessment

$$\frac{N_{Ed}}{N_{b,Rd}} \leq 1.0 \dots \frac{10\,202\text{ kN/m}}{15\,168.62\text{ kN/m}} = \mathbf{0.67} \leq \mathbf{1.0} \dots \text{cross-section passes}$$

Combination of axial compression and bending assessment

Cross-section characteristics	
E	210000 MPa
f_y	355 MPa
Material Characteristics	
A	$6.67 \times 10^{-2}\text{ m}^2$
I_y	$5.15 \times 10^{-3}\text{ m}^4$
I_z	$5.15 \times 10^{-3}\text{ m}^4$
$W_{pl,y}$	$1.67 \times 10^{-2}\text{ m}^3$
$W_{pl,z}$	$1.67 \times 10^{-2}\text{ m}^3$
Internal forces - Section 1	
N_{Ed}	10 202 kN
$M_{Ed,y}$	-615.07 kNm
$M_{Ed,z}$	356.09 kNm
Internal forces - Section 2	
N_{Ed}	10 202 kN
$M_{Ed,y}$	-615.07 kNm
$M_{Ed,z}$	211.77 kNm
Cross-sectional resistances	
N_{Rk}	23 678.50 kN
$M_{Rk,y}$	5 923.89 kN

Interaction coefficients	
k_{yy}	1.55
k_{zy}	0.93
k_{zz}	1.55
k_{yz}	0.93
C_{my}	1.01
C_{mz}	1.01
γ_{M1}	1

$$\frac{N_{Ed}}{\chi_y N_{Rk}} + k_{yy} \frac{M_{y,Ed}}{\chi_{LT} M_{y,Rk}} + k_{yz} \frac{M_{z,Ed}}{\chi_{LT} M_{z,Rk}} \leq 1$$

$$\frac{N_{Ed}}{\chi_z N_{Rk}} + k_{zy} \frac{M_{y,Ed}}{\chi_{LT} M_{y,Rk}} + k_{zz} \frac{M_{z,Ed}}{\chi_{LT} M_{z,Rk}} \leq 1$$

Section 1 ($x = 11 \text{ m}$):

$$\frac{10\,202}{\frac{0.64 \times 23\,678.50}{1}} + 1.55 \frac{615.07}{\frac{5\,923.89}{1}} + 0.93 \frac{356.09}{\frac{5\,923.89}{1}} = 0.89 \leq 1 \quad \text{PASSES}$$

$$\frac{10\,202}{\frac{0.64 \times 23\,678.50}{1}} + 0.93 \frac{615.07}{\frac{5\,923.89}{1}} + 1.55 \frac{356.09}{\frac{5\,923.89}{1}} = 0.86 \leq 1 \quad \text{PASSES}$$

Section 2 ($x = 3 \text{ m}$):

$$\frac{10\,202}{\frac{0.64 \times 23\,678.50}{1}} + 1.45 \frac{615.07}{\frac{5\,923.89}{1}} + 0.87 \frac{211.77}{\frac{5\,923.89}{1}} = 0.87 \leq 1 \quad \text{PASSES}$$

$$\frac{10\,202}{\frac{0.64 \times 23\,678.50}{1}} + 0.87 \frac{615.07}{\frac{5\,923.89}{1}} + 1.45 \frac{211.77}{\frac{5\,923.89}{1}} = 0.82 \leq 1 \quad \text{PASSES}$$

Cross-section *CHS 813/27 mm* is sufficient for the design.

Summary

From the geotechnical investigation, it was obvious that very soft soil is overlaying hard rock, which led me to the decision of predrilling the piles. If the piles are prebored and grouted tightness of the structure is ensured. From calibration of analytical models, I learned that in case that piles are driven too much, say twice more than was design depth, it has a great influence on internal forces. On the other hand, if the wall is only touching the rockhead, seepage should be modelled and tightness would not be ensured. In the design of construction phases wall deformations were reduced to 0.1 m, which is acceptable value. Distribution of internal forces is significantly different in all phases, therefore no phase can be omitted as this could cause collapse of the structure or non-acceptable deformations to it. In comparison of different analytical models differences in bending moment values could be observed. Comparison of two different analytical models showed that different soil modelling has great effect on internal forces, even though the shape of the bending curve is very similar, values obtained from PLAXIS software are much higher. For the design, highest obtained values were accounted in order to execute safe and conservative design. In this particular case, temperature has no great influence on the strut design, but in my opinion it should be always considered, as it depends on many different factors and the influence will vary for individual structures. Studying second order effects on the wall by non-linear model in Scia Engineer showed 10% increase on maximum bending moment of the cofferdam's wall. I find this value high enough to say that second order should not be neglected in this type of structures. All structural members were successfully designed and assessed according to corresponding Eurocodes.

Reference List

1. **Mott MacDonald.** *Geotechnical Interpretive Report.* Hong Kong : s.n., April 2014.
2. **Nippon Steel.** *Nippon Steel and Sumitomo Metal Corporation.* [Online] 2016.
<https://www.nssmc.com>.
3. **Konsmar.** [Online] <http://konsmar.com/pilinworks.html>.
4. **Gould, Tony.** VP Groundforce. [Online] May 2012.
<https://www.vpgroundforce.com/gb/media-hub/articles/groundforce-blog/may-2012/load-and-temperature-effects-for-hydraulic-struts/>.
5. **Chapman, K.R., Cording, E.J. and Schnabel, H., J r .** Performance of a braced excavations in granular and cohesive soils. Lafayette : s.n., 1972. pp. 271-293.
6. **FINE.** *Online Help Geo5/FEM.* [Online] <http://www.finesoftware.eu/help/geo5/>.
7. **Braja M. DAS, Khaled Sobhan.** *Principles of Geotechnical Engineering.* 2013.
8. **Schmitt, P.** "Estimating the coefficient of subgrade reaction for diaphragm wall and sheet pile wall design". 1995.
9. **EN 1993.** *Eurocode 3: Design of steel structures.* 2005.
10. **Google.** Google Maps. [Online] 2015. www.google.com/maps/.
11. **EN 1997.** *Eurocode 7: Geotechnical design, Design Approach 2.* 2004.
12. **Karl, Terzaghi.** *Theoretical Soil Mechanics.* s.l. : Wiley, 1943.

List of short cuts and symbols

S	strut (level)
AD	anthropogenic deposit
MD	marine deposit
CDG	completely decomposed granite
M-C	Mohr Coulomb material model
L-E	Linear Elastic material model
γ_{unsat}	unsaturated unit weight of soil
γ_{sat}	saturated unit weight of soil
c'	effective cohesion
ϕ'	effective angle of internal friction
E'	deformation modulus
ν'	poissons ratio
K_0	at-rest earth pressures coefficient
R_{int}	
α	coefficient of thermal expansion
E	elastic modulus of steel
A	area of strut
Δt	change in temperature
E_s	elastic modulus of steel
ΔT	change in temperature
nA_s	total area of struts acting against the wall of area A_w
A_w	cut of area of the wall
E	soil modulus of deformation

H	height of the wall
ν	Poisson's ratio
δ	deflection of the wall due to the load change
γ_c	unit weight of concrete
γ_s	unit weight of structural steel
LC	load case
FEM	finite element method
CHS	circular hollow section
SL	strut level
N_{cr}	critical force
N_{Ed}	design value of the applied axial force (tension or compression)
M_{Ed}	design value of the applied bending moment
N_{Rd}	bearing capacity of normal force
M_{Rd}	bearing capacity of bending moment
χ	axial buckling coefficient
χ_{LT}	bending buckling coefficient
k_h	modulus of subsoil reaction
f_y	yield strength of steel
A	cross-sectional area
W	section modulus
A_v	shear area
I	moment of inertia
d	diameter
t	thickness

γ_M	material resistance factor
$N_{c,Rd}$	design bearing capacity in axial compression
$M_{c,Rd}$	design bearing capacity in bending
M_{Ed}^{2nd}	design value of the second order bending moment
$N_{b,Rd}$	buckling bearing capacity
λ	relative slenderness
L_{cr}	critical length
V_{Ed}	design shear force
$V_{pl,Rd}$	plastic shear bearing capacity
k_{ij}	interaction factors

List of Annexes

Annex A

A.1 Geometry

A.1.1 Ground Plan

A.1.2 Section

A.2 Construction Sequence

Annex B

B.1 Bending Moments Comparison in All Phases